ISSN 0140-3818
SSSU 82

UNIVERSITY OF SOUTHAMPTON

DEPARTMENT OF SHIP SCIENCE

FACULTY OF ENGINEERING AND APPLIED SCIENCE

ANALYTICAL MODELLING CONCERNING ONSET OF DELAMINATION IN FRP BEAM PANELS

H.J. Phillips and R.A. Shenoi

Ship Science Report 82

March 1994

ANALYTICAL MODELLING CONCERNING ONSET OF DELAMINATION IN FRP BEAM PANELS

by

H. J. PHILLIPS

R. A. SHENOI

UNIVERSITY OF SOUTHAMPTON

DEPARTMENT OF SHIP SCIENCE

MARCH 1994

CONTENTS

1. INTRODUCTION.

Delaminations are among the most common defects in fibre reinforced plastic (FRP) composite materials and structures. They could arise either during fabrication of the structure or through accidental impact during service. Delamination involves the separation of individual layers that constitute the laminate. The stage at which delamination occurs within the laminate is dependent on the material properties, geometric characteristics and specifics of the laminate loading. The failure of a laminate as prompted by delamination can generally be divided into three stages (1), as illustrated in figure 1. These include: (a) initiation of delamination; (b) growth of delamination with or without the interaction with other associated modes such as matrix cracking; and (c) final failure of the laminate often by in-plane mechanisms.

The formation and propagation of delaminations in structures have been studied by several investigators. For example, the models of Choi et. al. (2) and Clark (3), applicable to line and point loading respectively, provide qualitative predictions of delamination sizes. The model of Grady and Sun (4) provides an estimate of delamination growth but requires *a priori* knowledge of the number and locations of the delaminations. Liu's model (5) shows the effect of bending stiffness mismatch between adjacent plies on delamination sizes. The models of Wu and Springer (6) and Finn and Springer (7), provide the locations, shapes and sizes of delaminations. Suemasu (8,9) has studied the effects of multiple delaminations on the compression buckling behaviour of composite panels using analytical and experimental models. Wang et. al. (10) have presented a mechanistic model to study the buckling stability and crack stability (i.e. delamination growth) in short fibre composites. These works have formed the basis for the preliminary study carried out with regard to delamination

damage tolerance in marine FRP structures. Additional references from a literature search can be found in Appendix AA.

The objects of this initial study are four-fold:

(a) to achieve an analytical modelling capability to characterise onset of delamination;

(b) to examine the relevance of fracture mechanics criteria in modelling propagation of delamination.

(c) to present preliminary results derived from the theoretical modelling.

(d) to correlate the analytically formulated solutions with experimental results from tests carried out in DRA, Dunfermline.

2. MODELLING OF THE DELAMINATION PROCESS.

Delamination growth alters the stress distribution in the laminate plies. As a result properties such as residual laminate stiffness, strength and fatigue life are also affected. Hence it is important to be able to calculate the stiffness of a laminate which has delaminated in order to assess its structural performance.

Stiffness reduction due to delamination.

To analyse stiffness loss due to delamination, a simple rule-of-mixtures analysis coupled with laminated plate theory (11) can be used. O'Brien (12) developed a method by which the stiffness of a laminate completely or partially delaminated can be calculated.

Equation (1) gives the stiffness of an arbitrary composite laminate, E_{LAM}, in terms of laminate thickness, t. The complete method is discussed in Appendix A1.

$$E_{LAM} = \frac{1}{[a_{11}]\,t} \qquad (1)$$

where: $[a_{11}]$ is the first element of the in-plane compliance matrix [a], described in Appendix A1.

If the laminate is symmetric, then the stiffness can be written as:

$$E_{LAM} = \frac{1}{[X_{11}]\,t} \qquad (2)$$

where: $[X_{11}]$ is the first element of the inverse extensional stiffness matrix $[A]^{-1}$ described in Appendix A1.

The stiffness of a laminate as shown in figure 2 containing one or more complete delaminations, E^*, can also be calculated from equation (3). The derivation is shown in detail in Appendix A2.

$$E^* = \frac{\sum_{j=1}^{m} E_j \, t_j}{t} \qquad (3)$$

where: m is the number of sublaminates formed by the delaminations.

E_j is the stiffness of sublaminate j.

t_j is the thickness of sublaminate j.

The sublaminate stiffnesses can be calculated either from equation (1) as a general case, or from equation (2) if the sublaminate is symmetrical or if the bending-extension coupling for that sublaminate can be neglected.

In addition, the stiffness of a partially delaminated laminate, E_p as shown in figure 3 can be calculated from equation (4). The details of the derivation are given in Appendix A3.

$$E_p = \frac{a}{b} \left[E^* - E_{LAM}\right] + E_{LAM} \qquad (4)$$

where: a is the width of the delaminated strips.

b is half the laminate width.

E^* is the stiffness of an equivalent laminate with complete delaminations.

E_{LAM} is the intact laminate stiffness.

Modelling of delamination under compressive loading.

The modelling undertaken follows standard approaches pertaining to beam panels under compression as documented, for example, by Moshaiov (13) and Chai et. al. (14). The case of a centrally loaded straight column as shown in figure 4, was considered where P is the load, L is the column length, x is the distance from one end and dx is an incremental distance in the x-direction.

The theory described in Appendix B1 utilises the force and moment equilibrium equations to yield an equation, shown below, which can be appled to all three parts (i=1,2,3) of the delaminated beam shown in figure 5.

$$w_i^{iv} + \lambda_i^2 w_i'' = 0 \qquad \textbf{(5)}$$

where:

$$\lambda_i^2 = \frac{P_i}{D_i^*} \quad ; \quad D_i^* = \frac{E t_i^3}{12(1-\nu^2)} \qquad \textbf{(6)}$$

and P_i is the axial force per unit length in the i^{th} part.

D_i^* is the stiffness of the i^{th} part.

t_i is the thickness of the i^{th} part.

E is the Young's modulus.

ν is the Poisson ratio.

The harmonic solutions to equation (6) are:

$$w_i = A_i \sin\lambda_i x_i + B_i \cos\lambda_i x_i + C_i x_i + D_i \qquad (7)$$

where: w_i is the deflection of the i^{th} part.

A_i, B_i, C_i and D_i can be found from the boundary conditions and continuity relationships. (Shown in Appendix B2).

x_i is the distance along the beam with x=0 at the left hand end of the beam shown in figure 5.

The ends of the beam are assumed to be clamped in this analysis. From axial strain compatibility, axial equilibrium conditions and moment equilibrium at the intersection of the parts, the following equation can be written for the limiting case:

$$\frac{\lambda_1 t_1^3}{6\sin\lambda_1 l_1}\cos\lambda_1 l_1 + \frac{\lambda_1 t_2^2 t_1}{6\sin\frac{\lambda_1 l_2 t_1}{2t_2}}\cos\frac{\lambda_1 t_1 l_2}{2t_2} + \frac{\lambda_1 t_3^2 t_1}{6\sin\frac{\lambda_1 l_3 t_1}{2t_3}}\cos\frac{\lambda_1 l_3 t_1}{2t_3} + \frac{t_1 t_2 t_3}{l_3} = 0 \qquad (8)$$

where: t_i is the thickness of part i (i=1,2,3).

l_i is the length of part i (i=1,2,3).

λ_1 is given in equation (6) when i=1.

The complete analysis is shown in Appendix B2.

Equation (8) can be used to find the critical value of λ_1, or λ_{cr}, which gives the critical value of stress for delamination buckling to occur which can be calculated from equations (9) and (10):

$$\lambda_{cr}^2 = \frac{P_{cr}}{D_1^*} \tag{9}$$

$$\sigma_{cr} = \frac{P_{cr}}{Area} \tag{10}$$

where: D_1^* is given in equation (6).
P_{cr} is the critical buckling force.
Area is the laminate width multiplied by the laminate thickness.

3. RELEVANCE OF FRACTURE MECHANICS.

Fracture mechanics has been frequently utilised to characterise the behaviour of cracks in metals but its involvement in composite applications is less common. Sumpter (15) has studied the use of fracture mechanics in the design process and materials selection procedure.

Probably, the most well-known fracture mechanics concept is that relating elastic stress intensity, K to the characteristic stress using the following equation:

$$K = Y \sigma \sqrt{\pi a} \qquad (11)$$

where: Y is a structural geometric factor.

σ is the characteristic stress.

a is a crack dimension.

It can be assumed that the crack will advance at a fixed value of K, K_c, which is a material property independent of crack length, geometry and working stress at which K_c is attained.

An alternative approach for the analysis of cracks involves the use of the elastic strain energy release rate, G.

$$G = \frac{1}{B}\frac{dU}{da} \qquad (12)$$

where: U is the structural energy available to allow crack advance.

B is the material thickness.

a is the crack length.

It is usually assumed that the new fracture surface would require a critical energy dissipation rate, R and that fracture would occur when G was greater than or equal to R. The value of G when G was equal to R was noted as G_c.

If a crack in a composite advances in a plane parallel to the fibre direction in unidirectional composite or between laminae in a laminate, G can be written in the form (15,16):

$$G = \frac{K^2}{(2E_xE_y)^{1/2}}\left[\left(\frac{E_x}{E_y}\right)^{1/2} - \nu_{xy} + \frac{E_x}{2G_{xy}}\right]^{1/2} \qquad (13)$$

where: E_x is the Young's modulus in the x-direction.

E_y is the Young's modulus in the y-direction.

G_{xy} is the shear modulus.

υ_{xy} is the major Poisson's ratio.

K is the elastic stress intensity.

For a composite where the crack grows transversly, a more complex analysis is required.

During this phase of the study, it was decided to restrict attention to a relatively simpler formulation of O'Brien (12) since data to validate the other equations was neither readily identified nor available.

O'Brien (12) used fracture criteria to obtain a relationship between the critical strain value, ε_c for delamination onset based on a knowledge of E_{LAM}, the laminate stiffness, E^*, the stiffness of a completely delaminated laminate, G_c, the critical strain energy release rate:

$$G_c = \frac{\epsilon^2 t}{2} [E_{LAM} - E^*] \qquad \textbf{(14)}$$

The derivation is given in Appendix C.

This method of calculating the critical strain value for delamination onset has been used in the systematic study of delaminated laminates which is discussed in the next section.

4. COMPUTATIONAL ASPECTS.

Stiffness Reduction.

A laminate program has been written by the first named author in order to calculate the laminate stiffnesses of perfect, partially and completely delaminated laminates. A flowchart of the program is shown in Appendix D. The program was validated by using an example from O'Brien (12) as a basis.

To verify the relationship stated in equation (3), an 11 ply laminate with a lay-up as given below was considered:

$$[\pm 30/\pm 30/90/\overline{90}]_S$$

Two delaminations were modelled in both -30/90 interfaces and are assumed to occur simultaneously. Using equation (3) E^* was found to be 0.69 E_{LAM} which is equal to that calculated by O'Brien. The values of E_j for each sublaminate were found; equation (1) was used for the outer two sublaminates [±30/±30] which are not symmetrical and equation (2) was used for the central [90/90/90] sublaminate which is symmetrical. From experiments, it was discovered that the interfaces did not cleanly delaminate in the sense that the delaminations shifted from one -30/90 interface across the 90-deg plies to the other -30/90 interface. This had the effect of reducing the bending-extension coupling. As a result, the bending-extension coupling in the two outer sublaminates was neglected and since the central /90/90/90/ sublaminate is symmetrical then each of the values of E_j can be calculated using equation (2) which yields the result, $E^* = 0.743\ E_{LAM}$ which is also equal to that calculated by O'Brien.

An attempt was then made to link the stiffness characteristics with critical strain levels to cause onset of delamination. This was done by using a transformed version of equation (14) and the data pertaining to G_c generated by O'Brien (12). The data was generated from experiments which were carried out on eighteen graphite-epoxy laminates with following configuration:

$$[\pm 30/\pm 30/90/\overline{90}]_s$$

The critical value of strain corresponding to delamination onset was calculated from the experimental applied stress and the laminate stiffness calculated from laminate plate theory. A value of 0.00347 was obtained and was entered into equation (14) to yield a value for critical strain energy release rate. A value of 137 J/m^2 was obtained and used in subsequent calculations for laminates with a similar material composition.

O'Brien (12) then made predictions of critical strain for delamination onset using the rearranged equation (14) for an alternative symmetric laminate with code $[+45_n/-45_n/0_n/90_n]_s$ (n=1,2,3). Hence, three laminate types were considered, namely those with 8 plies, 16 plies and 24 plies. Delaminations along both 0/90 interfaces and were compared with experimental values. The value for G_c used in equation (14) was that of 137 J/m^2. For all sublaminates, the bending-extension coupling matrix, [B], was neglected so equation (2) was used to calculate E for all sublaminates. The work by O'Brien was repeated and the results are shown in figure 6 which shows that the theoretical results obtained are equal to those obtained by O'Brien (12) and also data from Rodini and Eisenmann (17).

It is also noticed that in the thinner laminates, the delaminations will form at a higher nominal strain than the thicker laminates. It is, therefore necessary to yield a failure criterion which takes into account the thickness dependence of the delaminations. Hence, the strain energy release rate is a good parameter for predicting at which level of strain delamination is likely to occur.

After the program had been validated, a sensitivity study was carried out on the laminate with the following lay-up:

$$[\pm 30/\pm 30/90/\overline{90}]_s$$

The objective of this study was to investigate the effect on laminate stiffness and critical strain value for delamination onset, of the number of delaminations as well as their location.

The study was concerned entirely with laminates containing complete delaminations. The critical value of strain for delamination onset for each case was calculated from equation (14) and the stiffness values were calculated from equation (2). For the laminate shown in figure 7, with one delamination, graphs of location against laminate stiffness and critical strain are shown in figures 8a and 8b respectively. The axis labelled 'Delamination location' represents the ply number beneath which the delamination occurs. i.e. number 3 represents a delamination below ply 3 (between plies 3 and 4). It can be seen that the laminate stiffness and maximum critical strain for delamination onset occur for a delamination below ply 5 or ply 6, i.e. between two 90° plies. A laminate with one delamination below plies 4 or 7, i.e. in one of the -30/90 interfaces, gives rise to the lowest values of stiffness aswell as critical strain. The graphs shown in figures 8a and 8b also indicate that the values of laminate stiffness and critical strain onset for a laminate with one complete delamination

are symmetrical about the laminate neutral axis. This would be expected since the laminate in this example is symmetrical.

The laminate shown in figure 9 represents a laminate with two delaminations. Graphs of location of the second delamination against laminate stiffness and critical strain are shown in figures 10a and 10b respectively. In this particular case, the first delamination is assumed to be located between plies 1 and 2, in one of the +30/-30 interfaces. The second delamination is located first below ply 2, then ply 3, then ply 4 etc.. It is possible to see that the location of the second delamination does affect the stiffness and the critical strain value of the laminate.

Further studies were carried out on laminates with two delaminations. The study was systematically designed so as to include all possible location combinations of two delaminations in the 11 ply laminate. Figures 11a to 14b show the results. From the graphs it can be noted that the laminate with the lowest value of stiffness and critical strain is one with the delaminations below plies 3 and 8, i.e. in the two inner +30/-30 interfaces. This is shown in figures 12a and 12b respectively. A laminate with delaminations below plies 5 and 6, in the two 90/90 interfaces, gives rise to the highest values of laminate stiffness and critical strain. This is shown in figures 14a and 14b respectively.

Calculation of critical stress for laminate under compressive loading.

A program was written by the first named author to find the critical value of λ_1 in equation (8) which leads to a value of critical stress using equations (9) and (10). This was carried out by gradually increasing, from zero, the assumed value of λ_1 by small increments until the function in equation (8), which was originally positive, became negative. This was an important initial step as it gave an indication as to the shape of the function for different values of lambda. A typical graph of the function given in equation (8) versus λ_1 is shown in figure 15. Once the value of λ_1 which gave a negative value of the function had been reached, it was incremented by very small amounts to obtain a more accurate value of λ_1 using a Newton-Raphson solution method.

For a mid-thickness delamination, a specimen length of 3.0", a specimen thickness of 0.22" and material properties from (18), the results obtained were compared with those reported by (13). Initially, large differences were detected but it was discovered that the value of the increment to find λ_{crit} was too large and in fact the lowest, critical value of λ_1 was not being found. This became evident after a graph of the function against λ_1 was plotted out.

A plot of critical buckling stress against delamination length for a particular laminate with a symmetric delamination, i.e one where the delamination is at mid-depth, is shown in figure 16. The results also compare well with Wang et al. (18). The stiffness, E, in this case was taken as 1.58×10^6 psi (from the data in reference (18))

An attempt has been made to try and link up the stiffness reduction resulting from delamination with the modelling of

the compressive behaviour of a delaminated laminate. An initial study was carried out on a laminate with the following lay-up:

$$[\pm 30/\pm 30/90/\overline{90}]_S$$

Consider equation (8) above, and the diagram in figure 6, as well as the following parameters: thickness of part 1, T_1 = 0.22", thickness of part 2, T_2 = 0.11", thickness of part 3, T_3 = 0.11" and the total beam length, L = 3", where all dimensions are in inches. A critical value of λ_1 can be yielded from equation (8). Once this value has been calculated, then equation (9) yields D_1^* and equation (10) yields the value of critical stress, σ_{cr}. The value of E which is required to calculate D_1^* can be taken as three different values, namely, that of an intact specimen, E_{LAM} (equation (1) or (2)), that of a completely delaminated specimen, E^* (equation (3)) or that of a partially delaminated laminate, E_p (equation (4)). It has been assumed in this case that the beam shown in figure 3 can be idealised as the beam shown in figure 5. i.e that the strip delamination width a (fig 3) is comparable with the crack delamination length a ($=L_2/2$) in figure 5. The value of b, the laminate half-width was taken as L/2 in this case which is 1.5".

The complete analysis was carried out three times using three different values of E to calculate D_1^*.

Intact laminate	$E = 20 \times 10^6$ psi
Completely delaminated laminate	$E = 14.86 \times 10^6$ psi
Partially delaminated laminate	Depends on ratio a/b in equation (4).

The results of the analysis are shown in figure 17.

It can be observed that the critical stress values calculated using E for the intact laminate are higher than those calculated using E for the totally delaminated laminate, as would be expected. The values calculated using E for the partially delaminated laminate lie between the two, which again would be expected.

Systematic Study.

A systematic study was also carried out on delaminated specimens of total length 3.0 inches, Elastic modulus of 1.58×10^6 psi and a Poisson's ratio of 0.22. The delaminations in each case were considered to be symmetrical along the specimen length. The work was carried out to investigate the effect of:

(1) changing the through-the-thickness location of the delamination for a plate of constant thickness,

and

(2) changing the total plate thickness T_1 for a delamination at mid-thickness.

In each of the two cases, the delamination length was varied up to 1.25 inches. For the case when the delamination length equals zero, this indicates that the plate behaviour can be treated according to Euler theory. The critical buckling stress in this case can be calculated from the following equation, assuming clamped edges:

$$\sigma_{crit} = \frac{4\pi^2 D}{T_1 L^2} \qquad (15)$$

where: T_1 is the total specimen thickness.

L is the specimen length.

D is the beam stiffness, similar to that given in equation (6).

The results of study (1) are given in figure 18. From the graph it can be seen that the curves are of similar shape but that as the delamination approaches the plate mid-thickness ($T_2/T_1 = 0.5$), the curve becomes less pronounced. All five curves, however, level off as the delamination length increases. Also, all of the curves begin, as we would expect at the same value for a 'perfect' undelaminated plate for which the delamination length, a, equals zero.

The results for the second study are shown in two forms. Figure 19 shows the critical stress against delamination length for different values of plate thickness. This figure shows that the general shape of the curve is similar but that the slope becomes less pronounced for decreasing plate thickness, i.e that the critical stress becomes less dependent on delamintion length. Figure 20 shows the critical stress against plate thickness for different values of delamination length, a. This figure indicates that for increasing plate thickness the critical stress is more dependent on the delamination length, hence the wider spread of data on the right side of the graph.

Correlation with Experimental Data.

Experimental work has been carried out at DRA Dumfermline on two sets of beam specimens (19). The first series of beams were fabricated using a hand lay-up technique and the second were fabricated using a vacuum assisted resin transfer (V.R.T.) process. All the beams were tested in compression until failure occurred. The beams had the following dimensions and properties:

Gauge length:	240 mm	
Width:	50 mm	
Thickness:	Hand Lay-up	
	20 mm	
	V.R.T.	
	12.7 mm	
Longitudinal Compression Modulus:	Hand Lay-up	
	18824 MPa (2.73×10^6 psi)	
	V.R.T.	
	29597 MPa (4.29×10^6 psi)	

For each of the two series of beams, a delamination was built into the beam at five different through-thickness locations. In addition, for each of the through-thickness locations the length of the delamination was varied. The stress at which the first buckle occurred was noted in each case, as was the stress at which final failure was reached.

The beam dimensions, properties and loading conditions were entered into the computer code discussed above in an attempt to compare the theoretical results using equations (8), (9) and (10) with the experimental data. Figures 21a-21e and 22a-22d show the results.

For the hand lay-up specimens, in general the predictive model gives a reasonably accurate estimate of the critical buckling stress. The results are shown in figures 21a to 21e. When the depth of the in-built delamination is 0.8 mm below the outer surface (T_3 = 0.8 mm), it is observed that the model gives a curve whose data points are above the experimental values. When the depth of the delamination increases to 1.7 mm, 2.5 mm, 3.3 mm and 4.2 mm it is seen that the curve gradually falls below the experimental data points. The two extreme cases are shown in figures 21a and 21e. A possible explanation in the cases when the theoretical model lies below the experimental values is that the experimental values are those of "first buckle". It was pointed out by the experimentor that it was ensured that buckling was definitely occurring and that, in fact, buckling may have begun at a lower value.

The results for the V.R.T. specimens are shown in figures 22a to 22d. The theoretical curve lies, in general, above the experimental data points. The best fit to the data is obtained when the delamination is 1.06 mm below the surface (T_3 = 1.06 mm). This is shown in figure 22b.

5. CONCLUDING REMARKS.

The work discussed here presents a number of features associated with the delamination process. The first is that of laminate stiffness reduction which is an inherent effect of delamination. The analysis has been discussed, incorporated into an existing program and the results compared with existing data. An extension of this work yields an expression for critical strain value for delamination onset. Results obtained from this expression have been verified using existing data.

Secondly, a characteristic equation gives an analytical solution of the critical buckling load of delaminated plates. A program was written to yield results which agree favourably with those reported in previous papers and also compare well with a series of experimentally determined data points.

The next phase of the work will seek to consolidate the analytical models generated upto now and to extend the modelling capability. The envisaged tasks are:

a) to conduct a systematic study of the influence of lay-up on critical failure loads on beam panels,

b) to extend the modelling capability to cover plate panels,

c) to incorporate fracture mechanics criteria to predict the growth of delaminations using for instance, modified Paris-relationships,

d) to investigate the use of finite element analysis for investigating internal stress patterns in delaminated panels .

6. ACKNOWLEDGEMENTS.

The work outlined in this report has been funded jointly by SERC/MTD and MOD(PE).

7. REFERENCES.

[1] P. A. Lagace. 'Delamination - From Initiation to Final Failure'. Proceedings of the 9th International Conference on Composite Materials, ICCM/9, Madrid, 12-16 July, Volume I, pp 120-121.

[2] H. Y. Choi, H. Y. T. Wu, F. K. Chang. 'A new Approach toward Understanding Damage Mechanisms and Mechanics of Laminated Composites due to Low-Velocity Impact, Part II- Analysis'. Journal of Composite Materials, **25**, August 1991, pp 1012-1038.

[3] G. Clark. 'Modelling of Impact Damage in Composite Laminates'. Composites **20** (3), 1989, pp 209-214.

[4] J. E. Grady, C. T. Sun. 'Dynamic Delamination Crack Propogation in a Graphite-Epoxy Laminate'. Composite Materials: Fatigue and Fracture, ASTM STP 907, ed. H. T. Hahn, 1986, pp 5-31.

[5] D. Liu. 'Impact Induced Delamination - A view of Bending Stiffness Mismatching'. Journal of Composite Materials, **22**, July 1988, pp 674-692.

[6] H. T. Wu, G. S. Springer. 'Impact Induced Stresses, Strains and Delaminations in Composite Plates'. Journal of Composite Materials, **22**, June 1988, pp 533-560.

[7] S. R. Finn, G. S. Springer. 'Delaminations in Composite Plates under Transverse Static or Impact Loads- A model'. Composite Structures, **23** (3), 1993, pp 177-190.

[8] H. Suemasu. 'Postbuckling Behaviour of Composite Panels with Multiple Delaminations'. Journal of Composite Materials, **27** (11), 1993, pp 1077-1096.

[9] H. Suemasu. 'Effects of Multiple Delaminations on Compression Buckling Behaviour of Composite Panels'. Journal of Composite Materials, **27** (12), 1993, pp 1172-1192.

[10] S. S. Wang, N. M. Zahlan, H. Suemasu. 'Compressive Stability of Delaminated Random Short Fibre Composites, Part I- Modelling and Methods of Analysis'. Journal of Composite Materials, **19**, July 1985, pp 296-316.

[11] R. A. Shenoi & J. F. Wellicome (Eds.). Composite Materials in Maritime Structures, Volume 1. Cambridge University Press 1993.

[12] T. K. O'Brien. 'Characterization of Delamination Onset and Growth in a Composite Laminate'. Damage in Composite Materials, ASTM STP 775, K. L. Reifsnider, Ed. American Society for Testing and Materials, 1982, pp 140-167.

[13] A. Moshaiov & J. Marshall. 'Analytical Determination of the Critical Load of Delaminated Plates.' Journal of Ship Research, **35** (1), March 1991, pp. 87-90.

[14] H. Chai, C. D. Babcock & W. G. Knauss. 'One Dimensional Modeling of Failure in Laminated Plates by Delamination Buckling'. Int. J. Solids Structures, 1981, **17** (11), pp 1069-1083.

[15] J. D. G. Sumpter. 'Fracture Criteria for Naval composites: an initial review of the literature and proposals for further research'. DRA TM (AWMS) 92236, September 1992.

[16] G. C. Sih, P. C. Paris & G. R. Irwin. 'On Cracks in Rectilinearly Anisotropic Bodies'. International Journal of Fracture Mechanics, **1**, 1965, pp 189-203.

[17] B. T. Rodini and J. R. Eisenmann. Fibrous Composites in Structural Design, Plenum, New York, 1980, pp 441-457.

[18] S. S. Wang, N. M. Zahlan & H. Suemasu. 'Compressive Stability of Delaminated Random Short-Fibre Composites, Part II- Experimental and Analytical Results'. J. Composite Materials, **19**, July 1985, pp 317-333.

[19] Personal communication with researchers at DRA Dunfermline. March 1994.

APPENDICES.

APPENDIX AA. LITERATURE SEARCH.

The format for the search is summarised below:

NUMBER. AUTHOR

Title.

Reference.

- Main Points.

---

1. H. T. HAHN

A mixed mode fracture criterion for composite materials.

Composite Technology Review, Volume 5, 1983, pp 26-29.

- energy release rates (and critical values)
- stress intensity factors (and critical values)
- modes I and II considered i.e. mixed-mode.
- analytical solutions (simple equations)
- experimental correlation
- graphite/epoxy

2. B. J. LONG & S. R. SWANSON

Ranking of laminates for edge delamination resistance.

Composites, volume 25, number 3, 1994, pp 183-188.

- energy release rates
- finite element techniques (using gap elements)
- systematic study: various stacking sequences for $\pi/4$ quasi-isotropic laminates
- experimental correlation- tensile tests
- use 'modified virtual crack closure' technique
- modes I and II energy release rates
- carbon/epoxy

3. J. IVENS et. al.

2.5D fabrics for delamination resistant composite structures.

Composites, volume 25, number 2, 1994, pp 139-146.

- mode I double cantilever beam tests
- mode II end load split tests
- plain 2D glass fabric
- 2.5D fabrics with glass piles and epoxy resin
- 0 deg, 90 deg and 45 deg : tested in 3 orientations
- vary pile length and densities
- fracture toughness
- experimentation: modes I and II tests- fracture toughness
  calculations
  impact testing
  tensile testing
- critical strain energy release rates

4. J. WANG & B. L. KARIHALOO

Cracked composite laminates least prone to delamination.

Proceedings of the Royal Society of London A, volume 444, 1994, pp 17-35.

- vary ply angle, relative stiffness & thickness
- minimise stress intensity factors
- analytical solution (use Airy stress function and Bessel function)
- graphite/epoxy

5. A. GARG

Delamination- a damage mode in composite structures.

Enginnering Fracture Mechanics, volume 29, number 5, 1988, pp 557-584.

(A Review)

- delaminations: caused by interlaminar stresses near the free edge
- parametric study of variation in delamination onset strains with thickness (for 3 different lay-ups)
- delaminations: caused by impact
- experiments: impact tests
- graphite/PEEK
- graphitr/epoxy
- delamination: caused by matrix cracks
- EFFECT OF DELAMINATION:
- residual strength
- residual stiffness
- critical strain energy release rates
- critical buckling loads
- fracture toughness- calculation of (experimentally)

6. J. G. WILLIAMS

On the calculation of energy release rates for cracked laminates.

International Journal of Fracture 36, 1988, pp 101-119.

- analytical solution
- derive strain energy release rates from L.E.F.M
- modes I and II
- testing methods
- post initiation behaviour from system compliances

7. YIN & WANG

The energy release rate in the growth of a one-dimensional delamination.

Trans. of ASME, Journal of Applied Mechanics, volume 51, December 1984, pp 939-941.

- algebraic expression of energy release rate using J-integral method (in terms of post-buckling solution of delaminated plate)

8. ADAN et. al.

Buckling of multiply delaminated beams.

Journal of Composite Materials, volume 28, number 1, 1994, pp 77-90.

- analytical model for buckling
- prebuckling & buckling equations
- effects of crack length & location

9. BONIFACE et. al.

Strain energy release rates and the fatigue growth of matrix cracks in model arrays in composite laminates.

Proceedings of the Royal Society of London A, volume 432, 1991, pp 427-444.

- strain energy release rates: from compliance approach & energy method
- experimentation
- fatigue
- glass/epoxy
- theory/experimentatio correlation

10. MAHISHI & ADAMS

Energy release rates during delamination crack growth in notched composite laminates.

Delamination and Debonding of Materials. ASTM, STP 876, Ed. Johnson, W. S., American Society for Testing Materials, Philadelphia, 1985, pp 217-237.

- elastic strain energy release rates
- finite element
- initiation and growth

11. J. G. WILLIAMS

Fracture mechanics of composite failure.
(Review)

Proceeding of the Institute of Mechanical Engineers, volume 204, 1990, pp 209-218.

- critical stress intensity factors
- strain energy release rates
- modes I and II
- analytical
- double cantilever beam (DCB) test
- delamination cracking
- delamination under compression
- toughness
- postbuckling

12. WANG

Fracture mechanics for delamination problems in composite materials.

Journal of Composite Materials, volume 17, May 1983, pp 210-223.

- mixed-mode stress intensity factors
- strain energy release rate
- edge delaminated graphite/epoxy composites
- axial tension
- effects of fiber orientation, ply thickness & delamination length
- Lekhnitskii stress potentials
- Irwin's virtual crack extension concept

13. SUEMASU

Effects of multiply delaminations on compressive buckling behaviour of composite panels.

Journal of Composite Materials, volume 27, number 12, 1993, pp 1172-1192.

- analytical & experimental
- Rayleigh Ritz
- f.e analysis
- plain woven fabric glass/epoxy
- onset & postbuckling
- strain energy

14. SUEMASU

Postbuckling behaviors of composite panels with multiple delaminations.

Journal of Composite Mterials, volume 27, number 11, 1993,pp 1077-1096.

- analytical: Rayleigh Ritz
- contact problem for delaminated surfaces
- postbuckling behaviour
- experimental: compressive
- buckling load
- total energy release rate

15. GILLESPIE

Damage tolerance of composite structures: The role of interlaminar fracture mechanics.

Proceedings of the ninth International conference on Offshore mech. & arctic engineering, Houston, Texas, February 1990, pp 41-47.

- test methods: Modes I, II, III
- strain energy release rate
- virtual crack closure
- comparisons with experimental results

16. RYBICKI & KANNINEN

A finite element calculation of stress intensity factors by a modified crack closure integral.

Engineering Fracture Mechanics, volume 9, 1977, pp 931-938.

- stress intensity factors- modes I and II
- strain energy release rate
- finite element
- Irwin's crack closure integral

17. KIM & SONI

Experimental and analytical studies on the onset of delamination in laminated composites.

Journal of Composite Materials, volume 18, january 1984, pp 70-80.

- experimental
- graphite/epoxy
- applied uniaxial tension & compression
- analytical: average stress criterion
  max. stress criterion

18. RYBICKI, SCHMUESER & FOX

An energy release rate approach for stable crack growth in the free-edge delamination.

Journal of Composite Materials, volume 11, october 1977, pp 470-487.

- experimental and analytical
- boron/epoxy
- initiation & stable growth
- static tension loading
- finite element
- strain value for marked stiffness reduction
- energy release rates

19. IRWIN & KIES

Critical energy rate analysis of fracture strength.

Welding Journal Research supplement, april 1954, pp 193-s to 198-s

- strain energy release rates
- fracture tests

20. WANG, SLOMIANA & BUCINELL

Delamination crack growth in composite laminates.

Delamination and Debonding of Materials, ASTM, STP 876, Ed. Johnson W. S., American Society for Testing and Materials, Philadelphia, 1985, pp 135-167.

- energy method derived from fracture mechanics
- static & fatigue: compression & tensile
- experimental tests
- graphite/epoxy
- growth
- energy release rate method
- primplanted delaminations
- initiation

21. BATHIAS & LAKISMI

Delamination threshold and loading effect in fiber glass epoxy composite.

Delamination and Debonding of Materials, ASTM, STP 876, Ed. Johnson W. S., American Society for Testing and Materials, Philadelphia, 1985, pp 217-237.

- glass fiber/epoxy
- critical stress intensity factor & strain energy release rate
- fatigue growth
- effect of frequency, load ratio & overloads
- analytical & experimental

22. HIGHSMITH & REIFSNIDER

On delamination and the damage localisation process.

Fracture of Fibrous Composites, ASME, AMD-volume 74, 1986, pp 71-87.

- LEFM
- growth & initiation
- experimental & analytical
- graphite/epoxy laminates
- matrix cracking

23. BREWER & LAGACE

Quadratic stress criterion for initiation of delamination.

Journal of Composite Materials, volume 22, december 1988, pp 1141-1155.

- analytical & experimental
- graphite/epoxy
- initiation
- strain energy release rate
- average stress criterion
- tensile tests

24. HIGHSMITH & REIFSNIDER

Stiffness-reduction mechanisms in composite laminates.

Damage in Composite Materials, ASTM, STP 775, Ed. Refsnider, K. L., American Society for Testing and Materials, 1982, pp 103-117.

- analytical & experimental
- finite difference and shear lag models
- tension tests (static & tension-tension fatigue)
- transverse cracking (matrix cracking)

25. WILKINS et. al.

Characterising delamination growth in graphite-epoxy.

Damage in Composite Materials, ASTM, STP 775, Ed. Refsnider, K. L., American Society for Testing and Materials, 1982, pp 168-183.

- graphite/epoxy
- strain energy release rate
- experimental (modes I & II)
- static fracture, const. amplitude fatigue & spectrum fatigue
- f.e analysis
- preimplanted delaminations

26. O'BRIEN

Analysis of local delaminations and their influence on composite laminate behaviour.

Delamination and Debonding of Materials, ASTM, STP 876, Ed. Johnson W. S., American Society for Testing and Materials, Philadelphia, 1985, pp 282-297.

- strain energy release rate
- delaminations growing from matrix ply cracks
- previous experiments on graphite/epoxy
- delamination onset prediction
- edge delamination observed
- matrix ply cracks induced delamination
- local strain concentration analysis
- edge & local strain delamination

27. LIU, KUTLU & CHANG

Matrix cracking and delamination in laminated composite beams subjected to a transverse concentrated line load.

Journal of Composite Materials, volume 27, number 5, 1993, pp 436-470.

- analytical-stress analysis
- contact analysis
- failure analysis
- experiments
- matrix cracking & delamination
- non linear f.e method to solve equation for total potential energy
- prediction of initial failure
- crack propogation
- f.e to give strain energy release rates (modes I & II)
- comparisons with graphite/epoxy prepreg data (from experiments)
- flat panels, cylindrical panels

28. YEH & TAN

Buckling of elliptically delaminated composite plates.

Journal of Composite Materials, volume 28, number 1, 1994, pp 36-52.

- experimental & analytical
- non linear finite element program
- Newton-Raphson method
- mixed & global buckling behaviour
- effect of delamination region size, orientation of fiber direction, position of delaminated region in thickness direction & orientation of major axis of elliptic region with loading axis
- experiments
- carbon fibre reinforced prepregs
- elliptical teflon pieces
- f.e: shell elements

29. JAKUBOWSKI & REICHARD

Stiffness reduction of marine laminates due to cyclic flexing.

45th Annual Conference, Composites Institute, The Society of the Plastics Industry, Inc., 12-15 february 1990, pp 1-6, Session 8-E.

- experimental
- glass/polyester & glass/vinyl ester (non woven stitched)
- f.e analysis
- fatigue
- stiffness degradation
- f.e orthotropic theory
- ASTM methods use isotropic theory (60 % error)

30. KARDOMATEAS

End fixity effects on the buckling and post-buckling of delaminated composites.

Composites Science & Technology, volume 34, 1989, pp 113-128.

- analytical solution for post-buckling behaviour (using perturbation technique)
- energy release rate
- post-buckling solution and delamination characteristics
- critical buckling load

31. WHITCOMB

Finite element analysis of instability related delamination growth.

Journal of Composite Materials, volume 15, number 5, 1981, pp 403-426.

- postbuckled through-width delaminations
- experiments: fatigue tested
- stress distributions & strain energy release rates calculated
- effects of delamination lengths, delamination depths, applied loads & lateral deflections
- delamination growth behaviour (experimental)
- experimental- unidirectional epoxy/graphite
- teflon tape delamination
- static & fatigue
- modes I & II
- strain energy release rates

32. YIN

The effects of laminated structure on delamination buckling and growth.

Journal of Composite Materials, volume 22, June 1988, pp 502-517.

- postbuckling solutions
- energy release rates
- delamination growth
- critical strain for buckling onset
- effect on bending rigidity of angle of geometry axis and angle of loading axis
- thin film strip delamination
- mid-plane delamination in a symmetric laminate

33. WANG & SOCIE

Failure strength and damage mechanisms of E-glass/epoxy laminates under in-plane biaxial compressive deformation.

Journal of Composite Materials, volume 27, number 1, 1993, pp 40-58.

- E-glass/epoxy
- unidirectional and cross-ply specimens
- uniaxial and biaxial experiments
- critical buckling loads (theor. and expt'l)
- fractography
- strength criteria (Tsai-Hill & Tsai-Wu)

34. NAIRN & HU

The initiation and growth of delaminations induced by matrix microcracks in laminated composites.

International Journal of Fracture, volume 57, 1992, pp 1-24.

- analytical technique
- initiation & propogation of microcrack induced delaminations
- 2D stress analysis
- energy release rate for through-the-width delaminations
- 3D analysis
- carbon fibre/epoxy
- critical crack density

35. JOHANNESSON & BLIKSTAD

Fractography & fracture criteria of the delamination process.

Delamination and Debonding of Materials, ASTM, STP 876, Ed. Johnson W. S., American Society for Testing and Materials, Philadelphia, 1985, pp 411-423.

- graphite/epoxy laminates
- experiments (tension tests)
- stress intensity factors
- strain energy release rate
- vary lamination angle
- initiation of delamination
- ultimate failure

36. FINN & SPRINGER

Delamination in composite plates under transverse static or impact loads- a model.

Composite Structures, volume 23, number 3, 1993, pp 177-190.

- strain energy
- stress analysis
- finite element method
- predict delamination locations, shapes & sizes

37. FINN, HE & SPRINGER

Delamination in composite plates under transverse static or impact loads- experimenal results.

Composite Structures, volume 23, number 3, 1993, pp 191-204.

- to validate previous paper
- experiments
- graphite/epoxy (graphite-toughened epoxy & graphite/PEEK)
- effects of impactor velocity and impactor mass, material, thickness of back ply group, difference in fiber orientation between adjacent ply groups, plate thickness & impactor nose radius

38. MURTY & REDDY

Compressive failure of laminates and delamination buckling: a review.

Shock & Vibration Digest, volume 25, number 3, march 1993, pp 3-12.

- delamination initiation & growth
- fracture mechanics
- stress distributions
- strain energy release rates
- modes I & II
- preimpregnated delaminations:structure behaviour
- critical buckling loads
- circular plates with delaminations
- postbuckling behaviour
- delamination growth
- finite element

39. IRWIN

Fracture.

Handbuch der Physik, volume 6, 1958, pp 551-590.

Relevant section:

- crack-extension force
- strain energy release rate
- Weibull theory
- Griffith's proposal

40. SIMITSES, SALLAM & YIN

Effect of delamination of axially loaded homogeneous laminated plates.

American Institute of Aeronautics and Astronautics Journal, volume 23, number 9, september 1985, pp 1437-1444.

- analytical method
- predict delamination buckling loads
- effect of delamination position, size & thickness on critical loads for simple supports and clamped boundary conditions

41. O'BRIEN

Characterisation of delamintion onset & growth in a comp[osite laminate.

Damage in Composite Materials, ASTM, STP 775, Ed. Refsnider, K. L., American Society for Testing and Materials, 1982, pp 140-167.

- onset and growth of delaminations
- graphite/epoxy
- stiffness loss: analytical & experimental
- strain energy release rate
- critical strain values for delamination onset
- quasi-static loading
- delamination
- growth rates in fatigue
- finite element analysis

42. MOSHAIOV & MARSHALL

Analytical determination of the critical load of delaminated plates.

Journal of Ship Research, volume 35, number 1, march 1991, pp 87-90.

- analytical model
- predict critical load for delaminated plate buckling
- Rayleigh-Ritz
- compare with previous experimental data

43. CHAI, BABCOCK & KNAUSS

One dimensional modelling of failure in laminated plates by delamination buckling.

International Journal of Solids and structures, volume 17, number 11, 1981, pp 1069-1083.

- delamination growth
- strain energy release rate
- analytical
- delamination buckling

44. WANG, ZAHLAN & SUEMASU

Compressive stability of delaminated random short-fiber composites: Part I - modelling & methods of analysis.

Journal of Composite Materials, volume 19, july 1985, pp 296-316.

- analytical methods
- buckling stability & crack stability
- Rayleigh-Ritz
- finite element buckling analysis
- local & global buckling
- fracture mechanics
- SMC random fiber composites

45. WANG, ZAHLAN & SUEMASU

Compressive stability of delaminated random short-fiber composites: Part II - experimental & analytical results.

Journal of Composite Materials, volume 19, july 1985, pp 317-333.

- SMC random fiber composites
- pre-delaminated specimens
- influence of delamination length, crack position, number of delaminations and composite plate length on critical compressive stress & buckling modes
- crack growth
- strain energy release rate

46. KARDOMATEAS

Delamination growth during the initial postbuckling phase in composite plates.

Proceedings of the ninth International Conference on Composite Materials, ICCM/9, Madrid, 12-16 July 1993, Composites:Properties & Applications, volume VI, pp 479-486.

- initial postbuckling & growth
- perturbation procedure
- closed form solution for load & mid-point delamination deflection vs. applied compressive displacement
- energy release rates
- modes I & II
- stress intensity factors
- analytical solution

47. KONDO & SAWADA

Buckling & postbuckling analysis of delaminated composite plates.

Proceedings of the ninth International Conference on Composite Materials, ICCM/9, Madrid, 12-16 July 1993, Composites:Properties & Applications, volume VI, pp 463-470

- buckling & postbuckling behaviour of delmainted composite beam- plates
- compressive loading
- analytical solution & asymptotic solution
- potential energy release rates associated with delamination growth
- experiments
- buckling tests on isotropic aluminium alloy laminates with both ends clamped

48. MANIVASAGAM & CHANDRASEKARAN

Damage characterization and residual strength prediction of impacted composites.

Proceedings of the ninth International Conference on Composite Materials, ICCM/9, Madrid, 12-16 July 1993, Composites:Properties & Applications, volume VI, pp 44-50.

- analytical: characterize impact damage in terms of equivalent crack length
- strain energy release rate
- predict residual strength
- experimentation- low velocity impacts & 3-point bending
- isopthalic polyester/woven roving fibre glass
- unflawed specimens & specimens with straight cracks
- edgewise & flatwise conditions

49. LABONTE & WIGGENRAAD

Development of a structure relevant specimen for damage tolerance studies.

Proceedings of the ninth International Conference on Composite Materials, ICCM/9, Madrid, 12-16 July 1993, Composites:Properties & Applications, volume VI, pp 36-43.

- experimentation
- artificial delaminations
- compression loads
- C-scan damage areas & internal damage configuration determined
- heavily loaded wing panel model developed with soft skin, doublers & discrete

50. XIONG & POON

Prediction of residual compressive strength of impact-damaged composite laminates.

Proceedings of the ninth International Conference on Composite Materials, ICCM/9, Madrid, 12-16 July 1993, Composites:Properties & Applications, volume VI, pp 28-35.

- analytical midel
- predict compression-after-impact strength
- use sublaminate buckling approach to determine degradation of mechanical properties in damaged region
- simulate impact damage as soft inclusion & use complex potential method to determine stress redistribution
- point stress criterion used to predict the compression-after-impact strength
- experiments
- graphite fiber
- effect of orientation & aspect ratio of damage ellipse on residual compressive strength investigated analytically

51. KIMPARA et. al.

Fatigue damage accumulation and strength of CFRP laminates with different moduli and stacking sequences.

Proceedings of the ninth International Conference on Composite Materials, ICCM/9, Madrid, 12-16 July 1993, Composites:Behaviour, volume V, pp 31-38.

- carbon fibre/epoxy
- cross-ply & quasi-isotropic laminates
- experimentation:static tension & fatigue tension
- area of delamination and crack density related to stiffness degradation
- delamination onset under tension fatigue predicted using strain energy release rates
- effect of different moduli & stacking sequences

52. KYOUNG & KIM

Delamination buckling and growth of composite laminated plates with transverse shear deformation.

Proceedings of the ninth International Conference on Composite Materials, ICCM/9, Madrid, 12-16 July 1993, Composites:Properties & Applications, volume VI, pp 503-510.

- analytical model to determine delamination buckling load & growth
- axially loaded laminate beam-plate with through-the width delamination at an arbitrary location in loading direction
- effect of delamination size, depth & location on initial buckling
- strain energy release rate
- postbuckling state

53. SCZEPANIK-WEINMANN et. al.

Numerical and experimental 3D delamination behaviour of an anisotropic layered plate under compression loading.

Proceedings of the ninth International Conference on Composite Materials, ICCM/9, Madrid, 12-16 July 1993, Composites:Properties & Applications, volume VI, pp 736-743.

- theoretical & experimental
- carbon fibre/epoxy
- one through-width delamination
- theoretical values based on 3D finite element model
- geometrically non-linear analysis covering pre- and post-buckling
- fracture mechanics
- energy release rates
- modes I, II and III
- virtual crack closure method
- artificial delaminations (teflon)

54. LI & ARMANIOS

Effect of delaminations on an elastically tailored laminated composite plate.

Proceedings of the ninth International Conference on Composite Materials, ICCM/9, Madrid, 12-16 July 1993, Composites:Properties & Applications, volume VI, pp 728-735.

- closed form solution
- influence of free-edge delaminations on an elastically tailored composite plate
- analysis based on a shear deformation theory & a sublaminate approach
- graphite/epoxy
- analytical

55. VALOR et. al.

Compressive properties of woven fabric and/or glass fiber mat reinforced polyester laminates.

Proceedings of the ninth International Conference on Composite Materials, ICCM/9, Madrid, 12-16 July 1993, Composites:Properties & Applications, volume VI, pp 605-612.

- E-glass/unsaturated polyester
- continuous & CSM & plain woven roving fabric
- unidirectional & bidirectional models to predict the strength & stiffness in tension & compression
- effect of manufacturing process, number of layers, reinforcement type and percentage
- experimentation:side support in compression tests

56. KONIG et. al.

Delamination buckling: numerical simulation of experiments.

Proceedings of the ninth International Conference on Composite Materials, ICCM/9, Madrid, 12-16 July 1993, Composites:Properties & Applications, volume VI, pp 535-542.

- continuous carbon fibre/epoxy
- tension-compression fatigue tests
- measure delamination growth
- compute postbuckled states by a 2D plate finite element model
- artificial circular delamination

APPENDIX A. Estimation of Laminate Stiffness after Delamination.

APPENDIX A1. General Case.

$$\begin{bmatrix} [\epsilon^0] \\ [\kappa] \end{bmatrix} = \begin{bmatrix} [a] & [b] \\ [c] & [d] \end{bmatrix} \begin{bmatrix} [N] \\ [M] \end{bmatrix} \qquad \text{(A1)}$$

Classical laminate theory (11) yields the relationship:

where: $[\varepsilon^0]$ is the in-plane strains vector.
$[\kappa]$ is the plate curvatures vector.
[a] is the in-plane compliance matrix.
[b] is the coupling compliance matrix.
[d] is the flexural compliance matrix.
[N] is the in-plane forces vector.
[M] is the edge moments vector.

If N_x , the force per unit length in the x-direction is the only non-zero force then equation (A1) can be re-written as:

$$\varepsilon^0_x = a_{11} N_x \qquad \text{(A2)}$$

N_x is shown graphically in figure A1. Now, N_x is related to the direct in-plane stress in the x-direction, averaged across the laminate thickness, t as below:

$$\overline{\sigma_x} = \frac{N_x}{t} \qquad \text{(A3)}$$

Substituting equation (A3) into equation (A2) yields:

$$\epsilon_x^0 = a_{11}\,\overline{\sigma_x}\,t \tag{A4}$$

Now the stiffness E_x^0 can be written as :

$$E_x^0 = \frac{\overline{\sigma_x}}{\epsilon_x^0} \tag{A5}$$

Rearranging (A4) and substituting into (A5) gives the following equation for the stiffness of an arbitrary composite laminate, E_{LAM}.

$$E_{LAM} = \frac{1}{a_{11}\,t} \tag{A6}$$

where: a_{11} is the first element of the in-plane compliance matrix [a].

$[a] = [A]^{-1} + [A]^{-1}[B][D^*]^{-1}[B][A]^{-1}$

$[D^*] = [D] - [B][A]^{-1}[B]$

t is the laminate thickness.

also, for laminate with n plies:

$$A_{ij} = \sum_{k=1}^{n} [Q'_{ij}]_k\,(z_k - z_{k-1})$$

$$B_{ij} = \frac{1}{2}\sum_{k=1}^{n} [Q'_{ij}]_k\,(z_k^2 - z_{k-1}^2)$$

$$D_{ij} = \frac{1}{3} \sum_{k=1}^{n} [Q'_{ij}]_k \ (z_k^3 - z_{k-1}^3)$$

and

$$[Q'_{ij}]_k$$

is the reduced stiffness matrix for each ply k.

For a symmetric matrix, the coupling matrix [B] is equal to zero and equation (A6) can be written as:

$$E_{LAM} = \frac{1}{X_{11}\ t} \qquad \text{(A7)}$$

where: X_{11} is the first element in the matrix $[A]^{-1}$.

APPENDIX A2. Laminate Stiffness after Complete Delamination.

In the case of multiphase materials with n phases the following relationship holds:

$$E = \sum_{i=1}^{n} E_i \, V_i \qquad \text{(A8)}$$

where: E is the total elastic modulus of the multiphase material.

E_i is the modulus of phase number i.

V_i is the volume fraction of phase number i.

For a unidirectional material it can be assumed that volume fraction is proportional to thickness ratio (thickness of one phase to total laminate thickness), so equation (A8) can be written as:

$$E = \frac{1}{t} \sum_{i=1}^{n} E_i \, t_i \qquad \text{(A9)}$$

where: t is the total laminate thickness.
t_i is the thickness of phase number i.

If we assume that the laminate completely delaminates, as shown in figure A1, then we can assume that each sublaminate caused by the complete delaminations can be treated as a "phase j" in the above equations. Re-writing equation (A9) we have:

$$E^* = \frac{\sum_{j=1}^{n} E_j \, t_j}{t} \qquad \text{(A10)}$$

where: E^* is the stiffness of a completely delaminated laminate.

E_j is the stiffness of sublaminate number j.

t_j is the thickness of sublaminate number j.

t is the total laminate thickness.

APPENDIX A3. Laminate Stiffness due to Partial Delamination.

O'Brien (12) also developed an equation for the stiffness of a partially delaminated laminate, E_p. Figure A2 shows a laminate of width 2b with equal-sized delaminated strips width a along both edges. Using equation (A9) where each of the three parts of the laminate can be treated as three phases an equation for E_p can be formulated.

$$E_p = \frac{E_{LAM}(2b-2a) + E^*a + E^*a}{2b} \qquad \text{(A11)}$$

Rearranging equation (A11) yields O'Brien's relationship for a partially delaminated laminate.

$$E_p = \frac{a}{b}\,[E^*-E_{LAM}] + E_{LAM} \qquad \text{(A12)}$$

A more general form of equation (A12) can be derived, if it is assumed that the laminate stiffness loss and delamination size are related by equation (A13):

$$\frac{E_p - E_{LAM}}{E^* - E_{LAM}} = \frac{A}{A^*} \qquad \text{(A13)}$$

where: A is the delaminated area.
A^* is the total interfacial area.

Rearranging equation (A13) gives:

$$E_p = (E^* - E_{LAM})\frac{A}{A^*} + E_{LAM} \qquad \text{(A14)}$$

of which equation (A12) is a special case where $a/b = A/A^*$

APPENDIX B. Solution of a Compressively Loaded Laminated Beam with Delamination.

APPENDIX B1. Theoretical Considerations in order to yield an equation which describes the behaviour of a beam with a delamination.

The sign convention for positive moments and forces is shown in figure B1, where N and Q are the longitudinal and transverse components of force on the cross section, respectively. M is the bending moment.

From the diagram shown in figure B2, which represents the forces and moments acting on a column element in a deformed configuration, the following analysis can be carried out.

Summation of forces in the x-direction gives:

$$-N\cos\beta - Q\cos(90-\beta) + (N+dN)\cos(\beta+d\beta) + (Q+dQ)\cos(90-(\beta+d\beta)) = 0 \qquad \text{(B1)}$$

In order that the effect of rotations on the structure can be accounted for, the equlibrium equations are applied to the structure in a slightly deformed state. For a rotation, β, the square of the rotation is assumed to be small compared with unity. Therefore $\sin\beta$ is replaced by β and $\cos\beta$ replaced by 1.

Now,
$$\cos\beta = 1$$
$$\cos(90-\beta) = \sin\beta = \beta$$
$$\cos(\beta+d\beta) = 1$$
$$\cos(90-(\beta+d\beta)) = \sin(\beta+d\beta) = \beta+d\beta \qquad \text{(B2)}$$

Substituting equations (B2) into (B1) gives:

$$-N+(N+dN)-Q\beta+(Q+dQ)(\beta+d\beta)=0 \qquad \text{(B3)}$$

which reduces to:

$$\frac{dN}{dx} + Q\frac{d\beta}{dx} + \beta\frac{dQ}{dx} = 0 \qquad \text{(B4)}$$

Summation of forces in the z-direction gives:

$$N\sin\beta - Q\sin(90-\beta) - (N+dN)\sin(\beta+d\beta) + (Q+dQ)\sin(90-(\beta+d\beta)) = 0 \qquad \text{(B5)}$$

Substituting equations (B2) into (B5) gives:

$$N\beta - Q - (N+dN)(\beta+d\beta) + (Q+dQ) = 0 \qquad \text{(B6)}$$

which reduces to:

$$-N\frac{d\beta}{dx} - \beta\frac{dN}{dx} + \frac{dQ}{dx} = 0 \qquad \text{(B7)}$$

Summation of Moments gives:

$$M - (M+dM) + Qdx = 0$$

or,

$$Q = \frac{dM}{dx} \qquad \text{(B8)}$$

If we are considering slender beams, then transverse shearing stresses and forces are quite small. Therefore, we can assume that all quadratic terms representing non-linear interaction between small transverse and shearing forces and rotations may be neglected. The equilibrium equations (B4), (B7) & (B8) become:

$$\frac{dN}{dx} = 0 \qquad \text{(B9)}$$

$$\frac{dQ}{dx} - N\frac{d\beta}{dx} = 0 \qquad \text{(B10)}$$

$$Q = \frac{dM}{dx} \qquad \text{(B8)}$$

Substituting equation (B8) in (B10):

$$N' = 0 \qquad \text{(B11)}$$

$$M'' - N\beta' = 0 \qquad \text{(B12)}$$

Also, $$\beta = -w' \qquad \text{(B13)}$$

and $$M = -EIw'' \qquad \text{(B14)}$$

where:
' is the first differential w.r.t. x.
" is the second differential w.r.t. x.
w is the deflection in the z-direction.
E is the Young's Modulus.
I is the cross-section second moment of area.

Substituting equations (B13) and (B14) into (B12) we have:

$$(EIw'')'' - Nw'' = 0$$

and for constant EI,

$$EIw^{iv} - Nw'' = 0 \qquad \text{(B15)}$$

From equation (B11) it appears that N=constant in x, but from boundary conditions we see that for x=0,L, N=-P.

Hence, equation (B15) can be written as:

$$w^{iv} + \lambda^2 w'' = 0 \qquad \text{(B16)}$$

where:

$$\lambda^2 = \frac{P}{E\,I}$$

or in the case of a plate,

$$\lambda^2 = \frac{P}{D^*}$$

where:
$$D^* = \frac{Et^3}{12(1-\upsilon^2)} \qquad \text{(B17)}$$

and υ is the Poisson's ratio.

Equation (B16) applies to each of the three parts described in the main text.

So for the three parts, (i=1,2,3), the following equation holds:

$$w_i^{iv} + \lambda_i^2 w_i'' = 0 \qquad \text{(B18)}$$

where:

$$\lambda_i^2 = \frac{P_i}{D_i^*} \quad ; \quad D_i^* = \frac{Et_i^3}{12(1-\nu^2)} \qquad \text{(B19)}$$

and P_i is the axial force per unit length in the i^{th} part.
D_i^* is the stiffness of the i^{th} part.

APPENDIX B2. Complete solution to yield Characteristic Equation for Delaminated Beam Buckling.

The harmonic solutions to equation (B18) are:

$$w_i = A_i \sin\lambda_i x_i + B_i \cos\lambda_i x_i + C_i x_i + D_i \qquad \text{(B20)}$$

PART 1 (i=1)

Assuming both ends are clamped, then the following boundary conditions and continuity relationships can be used:

$$w_1 = 0 \text{ at } x_1 = 0 \quad \text{and} \quad w_1 = \delta \text{ at } x_1 = l_1 \qquad \text{(B21)}$$

$$w_1' = 0 \text{ at } x_1 = 0 \quad \text{and} \quad w_1' = \theta \text{ at } x_1 = l_1 \qquad \text{(B22)}$$

Differentiating equation (B20) gives:

$$w_i' = \lambda_i A_i \cos\lambda_i x_i - \lambda_i B_i \sin\lambda_i x_i + C_i \qquad \text{(B23)}$$

From the equations (B21) and (B22) we obtain the following relationships:

$$B_1 + D_1 = 0 \qquad \text{(B24)}$$

$$A_1 \sin\lambda_1 l_1 + B_1 \cos\lambda_1 l_1 + C_1 l_1 + D_1 = \delta \qquad \text{(B25)}$$

$$\lambda_1 A_1 + C_1 = 0 \qquad \text{(B26)}$$

$$\lambda_1 A_1 \cos\lambda_1 l_1 - \lambda_1 B_1 \sin\lambda_1 l_1 + C_1 = \theta \qquad \text{(B27)}$$

The constants can be found from equations (B24)-(B27):

From equations (B24) & (B26):

$$C_1 = A_1\lambda_1 \tag{B28}$$

$$D_1 = -B_1 \tag{B29}$$

Re-arranging equations (B30) and (B27):

$$B_1 = \frac{\delta - A_1[\sin\lambda_1 l_1 - \lambda_1 l_1]}{[\cos\lambda_1 - 1]} \tag{B30}$$

and,

$$B_1 = \frac{A_1\ [\lambda_1\cos\lambda_1 l_1 - \lambda_1] - \theta}{\lambda_1\sin\lambda_1 l_1} \tag{B31}$$

Equations (B30) and (B31) combine to give:

$$\frac{\delta - A_1\ [\sin\lambda_1 l_1 - \lambda_1 l_1]}{[\cos\lambda_1 l_1 - 1]} = \frac{A_1[\lambda_1\cos\lambda_1 l_1 - \lambda]}{[\lambda_1\sin\lambda_1 l_1]} - \theta \tag{B32}$$

So,

$$\delta\lambda_1\sin\lambda_1 l_1 - A_1[\lambda_1\sin\lambda_1 l_1][\sin\lambda_1 l_1 - \lambda_1 l_1]$$

$$= A_1[\cos\lambda_1 l_1 - 1][\lambda_1\cos\lambda_1 l_1 - \lambda_1] - \theta[\cos\lambda_1 l_1 - 1]$$

(B33)

and

$$\delta\lambda_1 \sin\lambda_1 l_1 + \theta[\cos\lambda_1 l_1 - 1]$$

$$= A_1[\lambda_1 \cos^2\lambda_1 l_1 - 2\lambda_1 \cos\lambda_1 l_1 + \lambda_1 + \lambda_1 \sin^2\lambda_1 l_1 - \lambda_1^2 l_1 \sin\lambda_1 l_1] \quad \text{(B34)}$$

and re-arranging gives:

$$A_1 = -\frac{[\delta \sin\lambda_1 l_1 + \frac{\theta}{\lambda_1}(\cos\lambda_1 l_1 - 1)]}{(\lambda_1 l_1 \sin\lambda_1 l_1 + 2\cos\lambda_1 l_1 - 2)} \quad \text{(B35)}$$

Substituting equation (B35) back into equation (B31) gives:

$$B_1 = -\frac{\delta \sin\lambda_1 l_1 - \frac{\theta}{\lambda_1}(\cos\lambda_1 l_1 - 1)}{(\lambda_1 l_1 \sin\lambda_1 l_1 + 2\cos\lambda_1 l_1 - 2)}(\lambda_1 \cos\lambda_1 l_1 - \lambda_1) - \theta}{\lambda_1 \sin\lambda_1 l_1}$$

(B36)

Re-arranging we have:

$$B_1 = -\frac{\delta(\cos\lambda_1 l_1 - 1)}{(\lambda_1 l_1 \sin\lambda_1 l_1 + 2\cos\lambda_1 l_1 - 2)}$$

$$-\frac{\frac{\theta}{\lambda_1}(\cos\lambda_1 l_1 - 1)(\lambda_1 \cos\lambda_1 - \lambda_1)}{\lambda_1 \sin\lambda_1 l_1 (\lambda_1 l_1 \sin\lambda_1 l_1 + 2\cos\lambda_1 l_1 - 2)} - \frac{\theta}{\lambda_1 \sin\lambda_1 l_1}$$

(B37)

Simplifying gives:

$$B_1 = -\frac{\delta(\cos\lambda_1 l_1 - 1)}{(\lambda_1 l_1 \sin\lambda_1 l_1 + 2\cos\lambda_1 l_1 - 2)}$$

$$-\frac{\theta(\cos^2\lambda_1 l_1 - 2\cos\lambda_1 l_1 + 1)}{\lambda_1 \sin\lambda_1 l_1 (\lambda_1 l_1 \sin\lambda_1 l_1 + 2\cos\lambda_1 l_1 - 2)} - \frac{\theta}{\lambda_1 \sin\lambda_1 l_1} \quad \text{(B38)}$$

and

$$B_1 = -\frac{\delta(\cos\lambda_1 l_1 - 1)}{(\lambda_1 l_1 \sin\lambda_1 l_1 + 2\cos\lambda_1 l_1 - 2)}$$

$$-\frac{\theta(\cos^2\lambda_1 l_1 - 1 + \lambda_1 l_1 \sin\lambda_1 l_1)}{\lambda_1 \sin\lambda_1 l_1 (\lambda_1 l_1 \sin\lambda_1 l_1 + 2\cos\lambda_1 l_1 - 2)} \quad \text{(B39)}$$

resulting in:

$$B_1 = \frac{-\delta(\cos\lambda_1 l_1 - 1)}{(\lambda_1 l_1 \sin\lambda_1 l_1 + 2\cos\lambda_1 l_1 - 2)}$$

$$+\frac{\theta}{\lambda_1}\frac{(\sin\lambda_1 l_1 - \lambda_1 l_1)}{(\lambda_1 l_1 \sin\lambda_1 l_1 + 2\cos\lambda_1 l_1 - 2)} \quad \text{(B40)}$$

Substituting equations (B28), (B29), (B35), (B40) into (B20) gives:

$$w_1 = -\frac{\left(\delta \sin\lambda_1 l_1 + \frac{\theta}{\lambda_1}(\cos\lambda_1 l_1 - 1)\right)}{(\lambda_1 l_1 \sin\lambda_1 l_1 + 2\cos\lambda_1 l_1 - 2)} \cdot \sin\lambda_1 x_1$$

$$- \frac{\delta(\cos\lambda_1 l_1 - 1)\cos\lambda_1 x_1}{(\lambda_1 l_1 \sin\lambda_1 l_1 + 2\cos\lambda_1 l_1 - 2)} + \frac{\theta}{\lambda_1} \frac{(\sin\lambda_1 l_1 - \lambda_1 l_1)\cos\lambda_1 x_1}{(\lambda_1 l_1 \sin\lambda_1 l_1 + 2\cos\lambda_1 l_1 - 2}$$

$$+ \lambda_1 x_1 \frac{\left(\delta \sin\lambda_1 l_1 + \frac{\theta}{\lambda_1}(\cos\lambda_1 l_1 - 1)\right)}{(\lambda_1 l_1 \sin\lambda_1 l_1 + 2\cos\lambda_1 l_1 - 2)}$$

$$+ \frac{\delta(\cos\lambda_1 l_1 - 1)}{(\lambda_1 l_1 \sin\lambda_1 l_1 + 2\cos\lambda_1 l_1 - 2)} - \frac{\theta}{\lambda_1} \frac{(\sin\lambda_1 l_1 - \lambda_1 l_1)}{(\lambda_1 l_1 \sin\lambda_1 l_1 + 2\cos\lambda_1 l_1 - 2}$$

(B41)

and re-arranging gives:

$$w_1 = \frac{1}{(\lambda_1 l_1 \sin\lambda_1 l_1 + 2\cos\lambda_1 l_1 - 2)} \times$$

$$\frac{\theta}{\lambda_1}[s\lambda_1 x_1 - c\lambda_1 l_1 s\lambda_1 x_1 + s\lambda_1 l_1 c\lambda_1 x_1 - \lambda_1 l_1 c\lambda_1 x_1 + \lambda_1 x_1 c\lambda_1 l_1 - \lambda_1 x_1 - s\lambda_1 l_1 + \lambda_1 l$$

$$+ \frac{1}{(\lambda_1 l_1 \sin\lambda_1 l_1 + 2\cos\lambda_1 l_1 - 2)} \times$$

$$\delta[c\lambda_1 l_1 - 1 + \lambda_1 x_1 s\lambda_1 l_1 - c\lambda_1 l_1 c\lambda_1 x_1 + c\lambda_1 x_1 - s\lambda_1 l_1 s\lambda_1 x_1] \quad \text{(B42)}$$

where:

$$c = \cos$$
$$s = \sin$$

Chai et al. (14) showed that δ and θ could be related by the following equation:

$$\delta = \frac{\theta}{\lambda_1}\tan\frac{\lambda_1 l_1}{2} \tag{B43}$$

also using a trigonometric identity:

$$\delta = \frac{\theta}{\lambda_1}\tan\frac{\lambda_1 l_1}{2} = \frac{\theta}{\lambda_1}\left(\frac{1-\cos\lambda_1 l_1}{\sin\lambda_1 l_1}\right) \tag{B44}$$

Substituting equation (B44) into (B42) gives:

$$w_1 = \frac{1}{(\lambda_1 l_1 \sin\lambda_1 l_1 + 2\cos\lambda_1 l_1 - 2)} \times$$

$$\frac{\theta}{\lambda_1}[s\lambda_1 x_1 - c\lambda_1 l_1 s\lambda_1 x_1 + s\lambda_1 l_1 c\lambda_1 x_1 - \lambda_1 l_1 c\lambda_1 x_1 + \lambda_1 x_1 c\lambda_1 l_1 - \lambda_1 x_1 - s\lambda_1 l_1 + \lambda_1 l$$

$$+ \frac{\theta}{\lambda_1}\frac{c\lambda_1 l_1 - c^2\lambda_1 l_1 - 1 + c\lambda_1 l_1 + \lambda_1 x_1 s\lambda_1 l_1 c\lambda_1 l_1}{\sin\lambda_1 l_1}$$

$$- \frac{\theta}{\lambda_1}\frac{c\lambda_1 l_1 c\lambda_1 x_1 + c^2\lambda_1 l_1 c\lambda_1 x_1 + c\lambda_1 x_1 - c\lambda_1 l_1 c\lambda_1 x_1}{\sin\lambda_1 l_1}$$

$$- \frac{\theta}{\lambda_1}\frac{s\lambda_1 l_1 s\lambda_1 x_1 + c\lambda_1 l_1 s\lambda_1 l_1 s\lambda_1 x_1}{\sin\lambda_1 l_1} \tag{B45}$$

which simplifies to :

$$w_1 = \frac{1}{(\lambda_1 l_1 \sin\lambda_1 l_1 + 2\cos\lambda_1 l_1 - 2)} \frac{\theta}{\lambda_1 \sin\lambda_1 l_1} \times$$

$$(2c\lambda_1 x_1 - \lambda_1 l_1 s\lambda_1 l_1 c\lambda_1 x_1 + \lambda_1 l_1 s\lambda_1 l_1 - 2 + 2c\lambda_1 l_1 - 2c\lambda_1 l_1 c\lambda_1 x_1)$$

(B46)

or:

$$w_1 = - \frac{\theta}{(\lambda_1 \sin\lambda_1 l_1)} (\cos\lambda_1 x_1 - 1) \qquad \text{(B47)}$$

PARTS 2 & 3 (i=2,3)

Similarly for parts 2 & 3 the following conditions and relationships can be applied:

$$w_i = \delta \quad at \quad x_i = -\frac{l_i}{2}, \; i = 2,3 \qquad \text{(B48)}$$

$$w_i' = \theta \quad at \quad x_i = -\frac{l_i}{2}, \quad i = 2,3$$

and

$$w_i' = 0 \quad at \quad x_i = 0, \quad i = 2,3 \qquad \text{(B49)}$$

$$w_i''' = 0 \quad at \quad x_i = 0, \quad i = 2,3$$

Using the above conditions, the following equations are yielded:

$$\lambda_i A_i + C_i = 0 \tag{B50}$$

$$-\lambda_i^3 A_i = 0$$

Hence, $$A_i = 0;\ C_i = 0 \tag{B51}$$

$$B_i = \frac{\theta}{\lambda_i \sin\lambda_i \frac{l_i}{2}} \quad i = 2,3 \tag{B52}$$

Also,

$$D_i = \delta - \frac{\theta \cos\lambda_i \frac{l_i}{2}}{\lambda_i \sin\lambda_i \frac{l_i}{2}} \quad i = 2,3 \tag{B53}$$

Substituting equations (B51), (B52) and (B53) into equation (B20) and re-arranging gives:

$$w_i = \frac{\theta}{\lambda_i \sin\lambda_i \frac{l_i}{2}} \left[\cos\lambda_i x_i - \frac{\cos\lambda_i l_i}{\cos\lambda_i \frac{l_i}{2}} \right] \quad i = 2,3 \tag{B54}$$

From axial strain considerations:

$$\frac{-(1 - \nu^2) P_3 l_3}{E t_3} + \frac{1}{2} \int_{\frac{-l_3}{2}}^{\frac{l_3}{2}} (w_3')^2 dx_3$$

$$= \frac{-(1 - \nu^2) P_2 l_2}{E t_2} + \frac{1}{2} \int_{\frac{-l_2}{2}}^{\frac{l_2}{2}} (w_2')^2 dx_2 + K\theta \tag{B55}$$

where:

$$K = t_1 - \frac{t_2}{2} - \frac{t_3}{2} \tag{B56}$$

Before buckling occurs the following equation holds:

$$(w_i')^2 \rightarrow 0, \quad i = 2,3 \tag{B57}$$

also,

$$\theta \rightarrow 0 \tag{B58}$$

Combining equations (B55), (B57) and (B58) gives:

$$P_3 = \frac{t_3}{t_2} P_2 \tag{B59}$$

Also,

$$P_i = \frac{t_i \, P_1}{t_1} \tag{B60}$$

Using the priciple of moment equilibrium:

$$M_1 = M_2 + M_3 - F_2 + F_3 \tag{B61}$$

Figure B3 shows the forces acting on parts 2 and 3 of the delaminated beam. Now, from the diagram it can be shown that:

$$F_2 = P_2 \left[\frac{t}{2} - \frac{(t - h)}{2}\right] = P_2 \frac{t_3}{2} \qquad \text{(B62)}$$

and

$$F_3 = P_3 \left[\frac{t}{2} - \frac{h}{2}\right] = P_3 \frac{t_2}{2} \qquad \text{(B63)}$$

Substituting equations (B62) and (B63) into equation (B61) gives:

$$M_1 = M_2 + M_3 - P_2 \frac{t_3}{2} + P_3 \frac{t_2}{2} \qquad \text{(B64)}$$

Also,

$$M_i = D_i \, w_i''\big|_{x_i = l_i} \qquad \text{(B65)}$$

Substituting equations (B47, B54, B55 & B65) into (B64) gives:

$$\frac{\lambda_1 t_1^3}{6 \sin \lambda_1 l_1} \cos \lambda_1 l_1 + \frac{\lambda_2 t_2^3}{6 \sin \frac{\lambda_2 l_2}{2}} \cos \frac{\lambda_2 l_2}{2}$$

$$+ \frac{\lambda_3 t_3^3}{6 \sin \frac{\lambda_3 l_3}{2}} \cos \frac{\lambda_3 l_3}{2} + \frac{t_1 t_2 t_3}{l_3} = 0 \qquad \text{(B66)}$$

From equations (B19) and (B60) it can be shown that:

$$\frac{\lambda_1}{\lambda_i} = \frac{t_i}{t_1}, \qquad i = 2,3 \tag{B67}$$

Substituting equation (B67) into (B66) gives:

$$\frac{\lambda_1 t_1^3}{6\sin\lambda_1 l_1}\cos\lambda_1 l_1 + \frac{\lambda_1 t_2^2 t_1}{6\sin\frac{\lambda_1 l_2 t_1}{2t_2}}\cos\frac{\lambda_1 t_1 l_2}{2t_2} + \frac{\lambda_1 t_3^2 t_1}{6\sin\frac{\lambda_1 l_3 t_1}{2t_3}}\cos\frac{\lambda_1 l_3 t_1}{2t_3}$$

$$+ \frac{t_1 t_2 t_3}{l_3} = 0 \tag{B68}$$

Equation (B68) can be simplified for the case of a symmetric delamination ie. when the delamination is at mid-thickness. In this case $t_1 = 2t_2 = 2t_3 = t$ where t is the total laminate thickness.

APPENDIX C. Strain Energy Release Rate and Failure Strain.

Strain energy release rate can be defined using the following equation:

$$G = \frac{dW}{dA} - \frac{dU}{dA} \qquad \text{(C1)}$$

where: $\frac{dW}{dA}$ is the Rate of Work Done.

$\frac{dU}{dA}$ is the Rate at which elastic Strain Energy is stored.

A is the flaw area.

Now, assuming that a nominal strain, ε, is sufficient to extend the flaw, then the work term vanishes and equation (C1) can be written as:

$$G = -V \frac{\epsilon^2}{2} \frac{dE}{dA} \qquad \text{(C2)}$$

where: V is the volume of the laminate(=2blt).

Now, by differentiating equation (A14) we obtain:

$$\frac{dE}{dA} = \frac{(E^* - E_{LAM})}{A^*} \qquad \text{(C3)}$$

and $$A^* = 2bl \qquad \text{(C4)}$$

where: l is the length of the laminate.

Substituting equations (C3) & (C4) into equation (C2) gives:

$$G = \frac{\epsilon^2 \, t}{2} [E_{LAM} - E^*] \qquad \text{(C5)}$$

O'Brien carried out tension tests on the 11 ply laminate mentioned above, in order to calculate the critical strain energy release rate, G_c from equation (C5) using the critical value of strain, ϵ_c, for delamination onset. It was suggested that G_c may be independent of the ply orientations that make up the delaminating surfaces. In order to investigate this, the value of G_c calculated from the 11 ply tests was used to calculate the critical strain values for delamination onset in other laminates. Re-arranging equation (C5) gives an equation for critical strain:

$$\epsilon_c = \sqrt{\frac{2 \, G_c}{t(E_{LAM} - E^*)}} \qquad \text{(C6)}$$

where: E_{LAM} is the laminate stiffness.

E^* is the stiffness of a completely delaminated laminate.

t is the laminate thickness.

APPENDIX D. FLOWCHART OF LAMINATE PROGRAM TO CALCULATE LAMINATE STIFFNESSES.

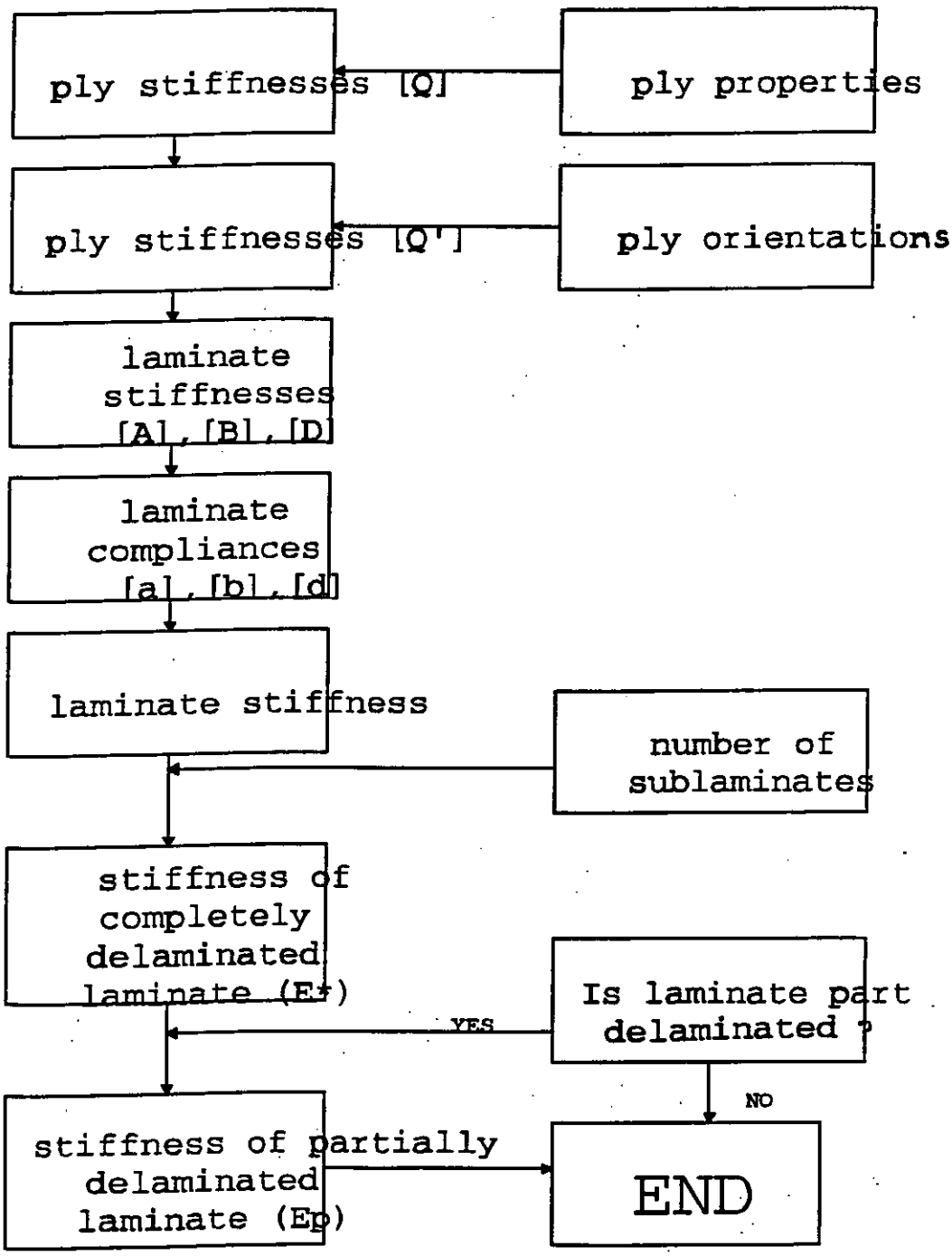

FIGURE 1. Stages of delamination failure.

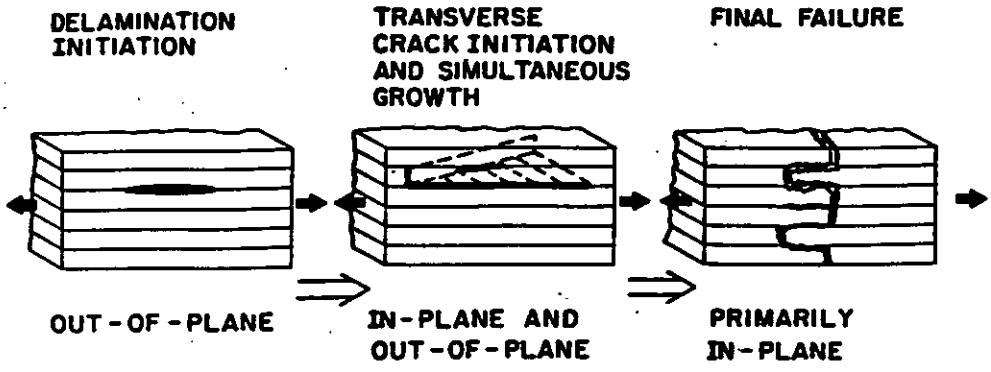

FIGURE 2. Laminate containing complete delaminations.

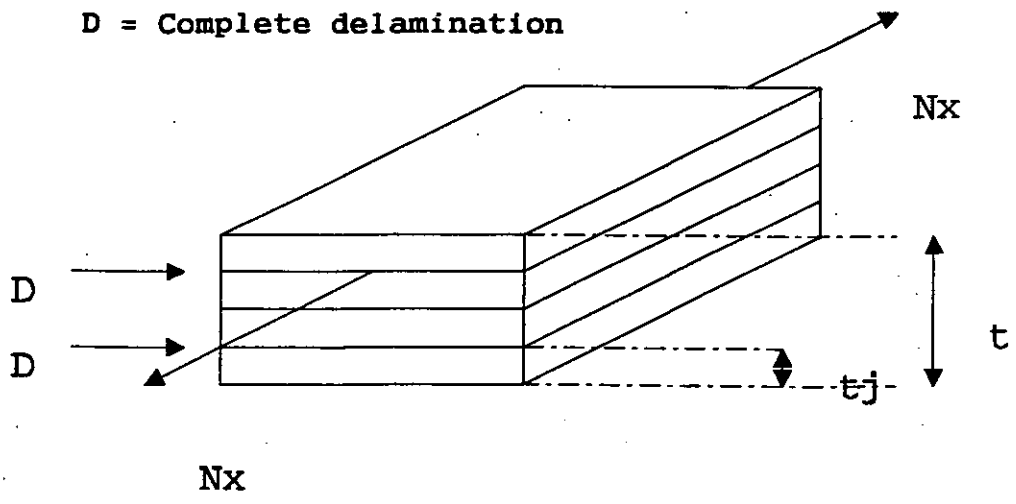

FIGURE 3. Laminate containing partial (edge) delaminations.

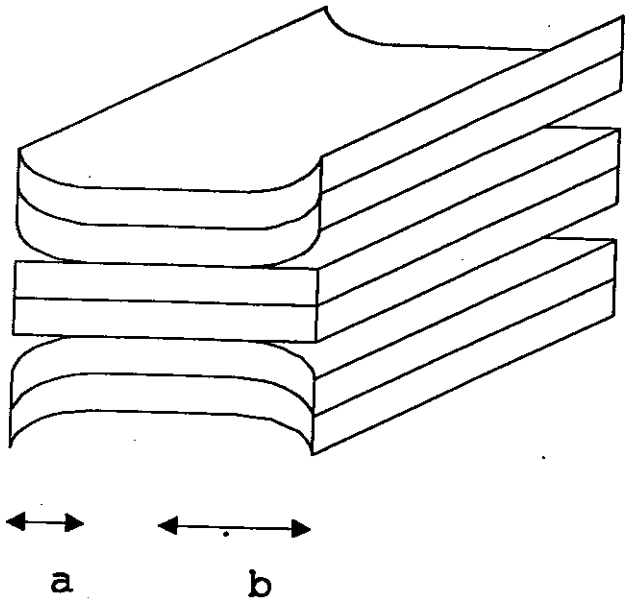

FIGURE 4. Centrally loaded straight column.

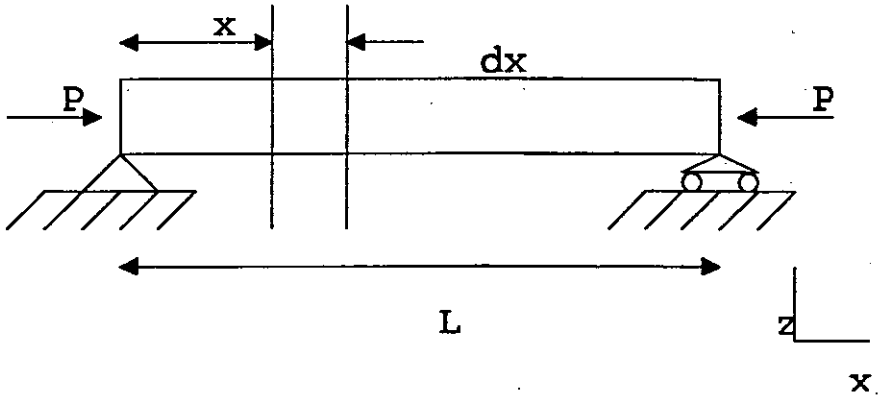

FIGURE 5. Model of three parts of a delaminated beam.

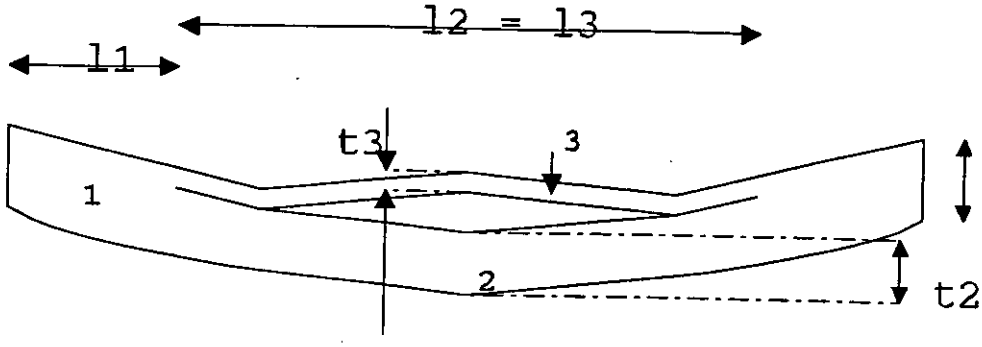

FIGURE 6. Critical strain for delamination onset against the number of plies.

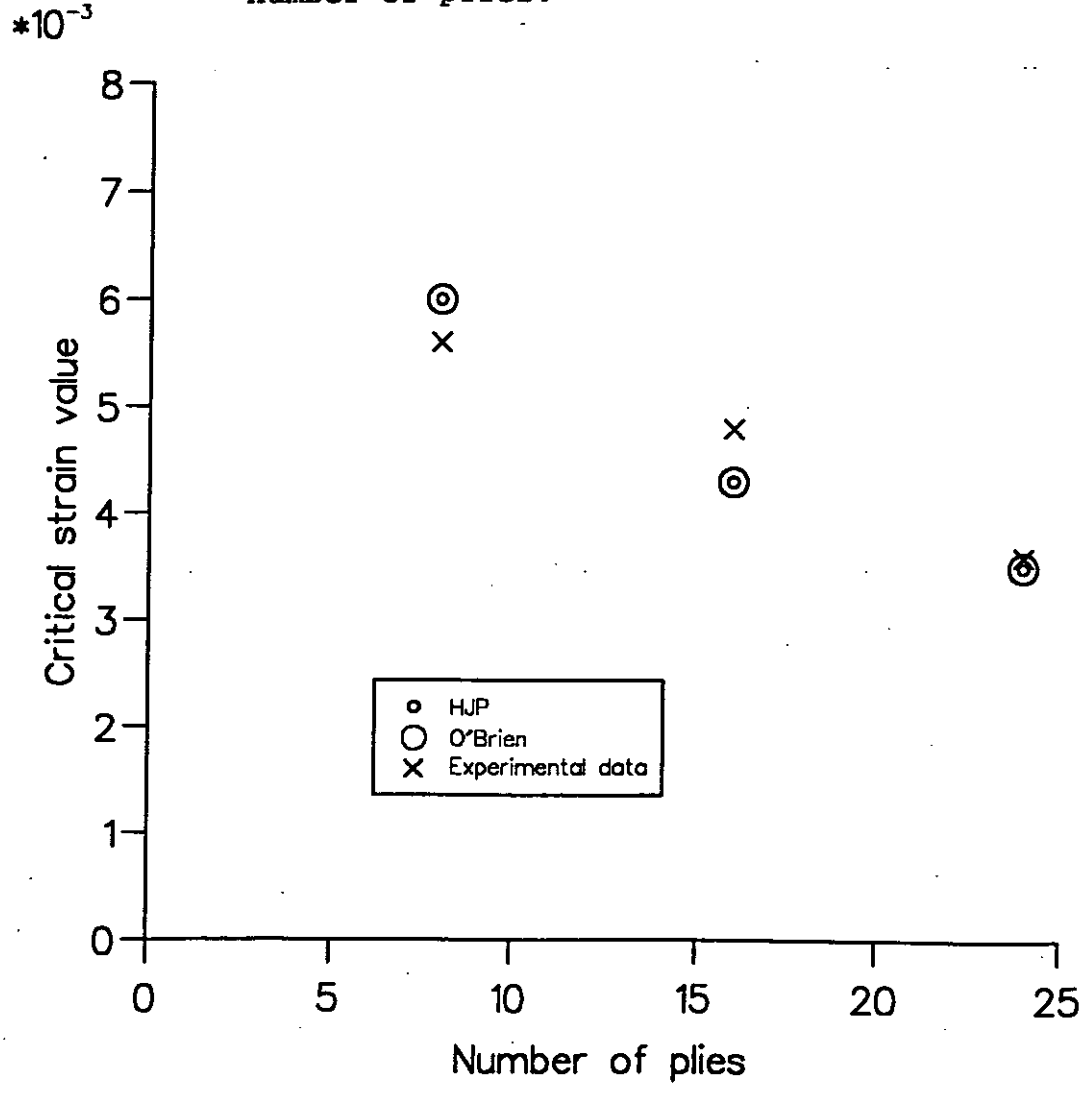

FIGURE 7. Laminate with one delamination.

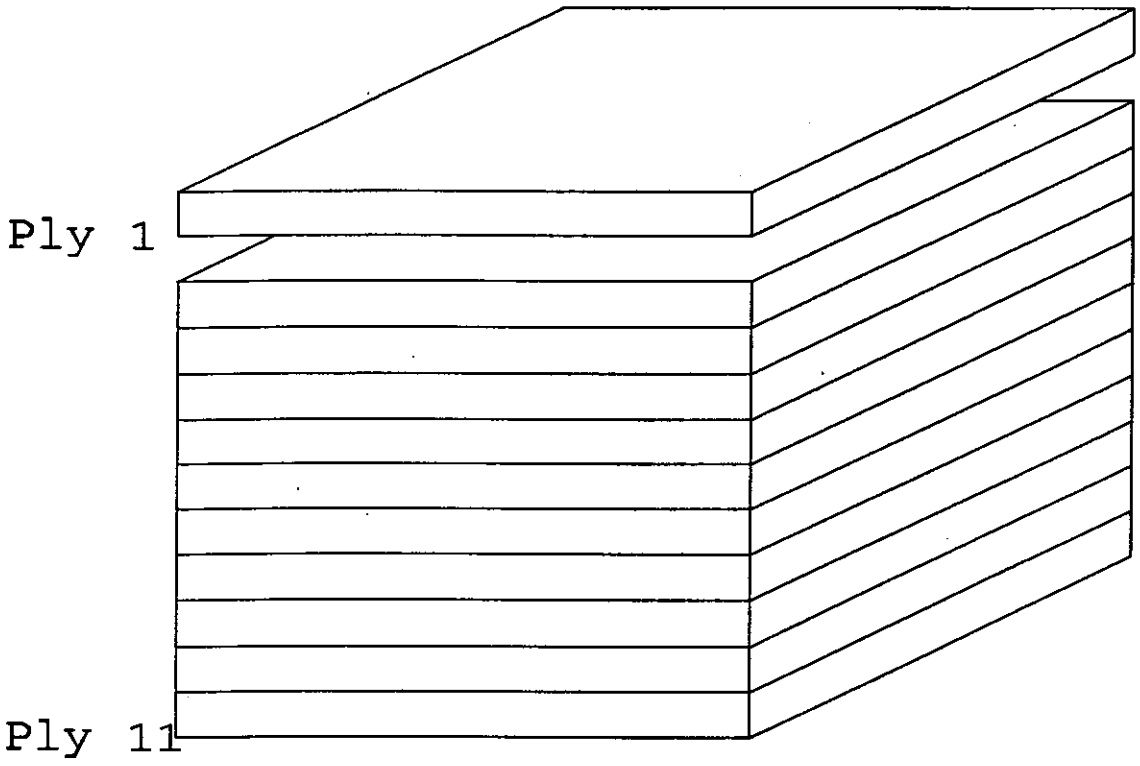

FIGURE 8a. The effect of location on the stiffness of a laminate with one delamination.

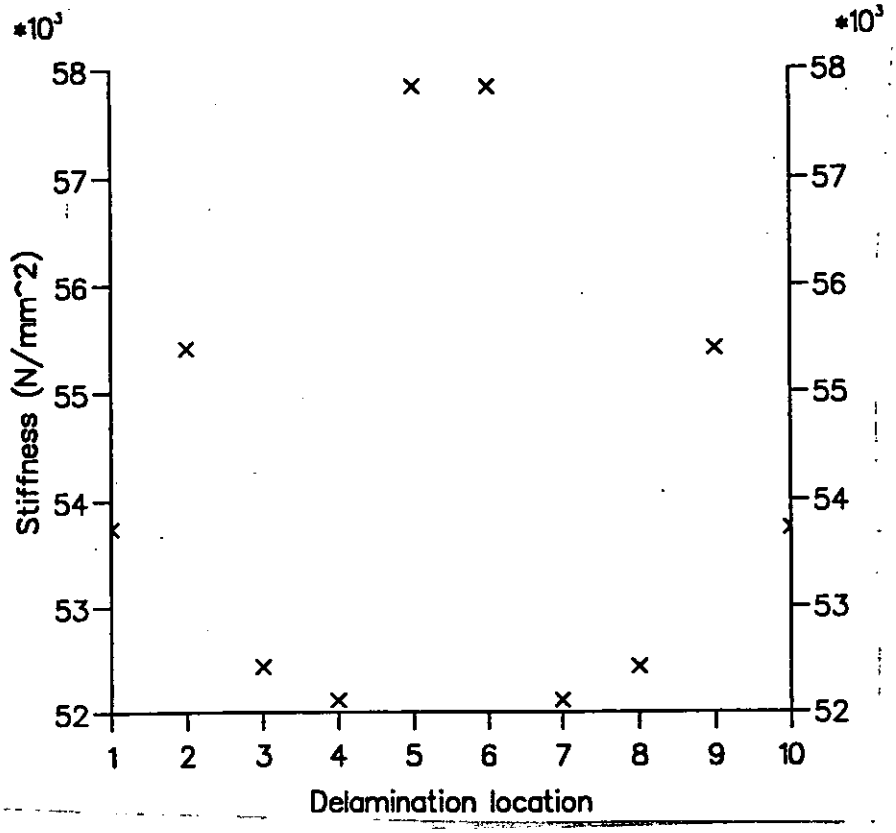

FIGURE 8b. The effect of location on the critical strain for delamination onset of a laminate with one delamination.

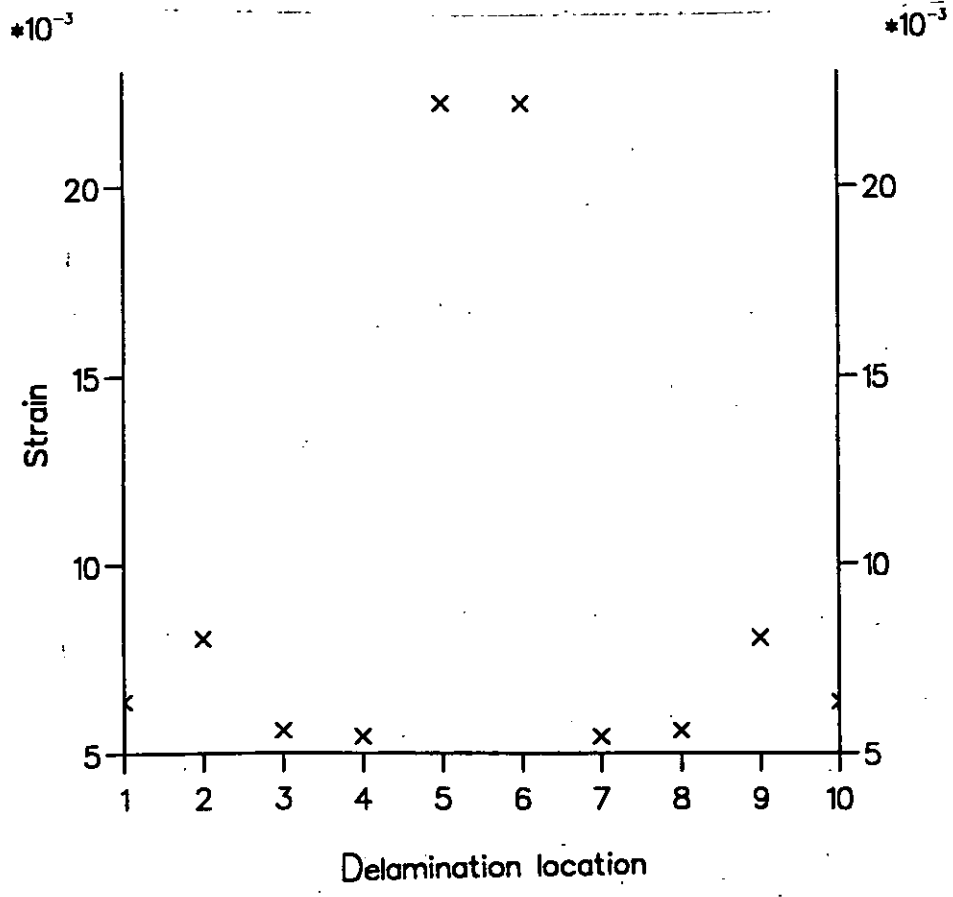

FIGURE 9. Laminate with two delaminations:
- first delamination is below ply 1.

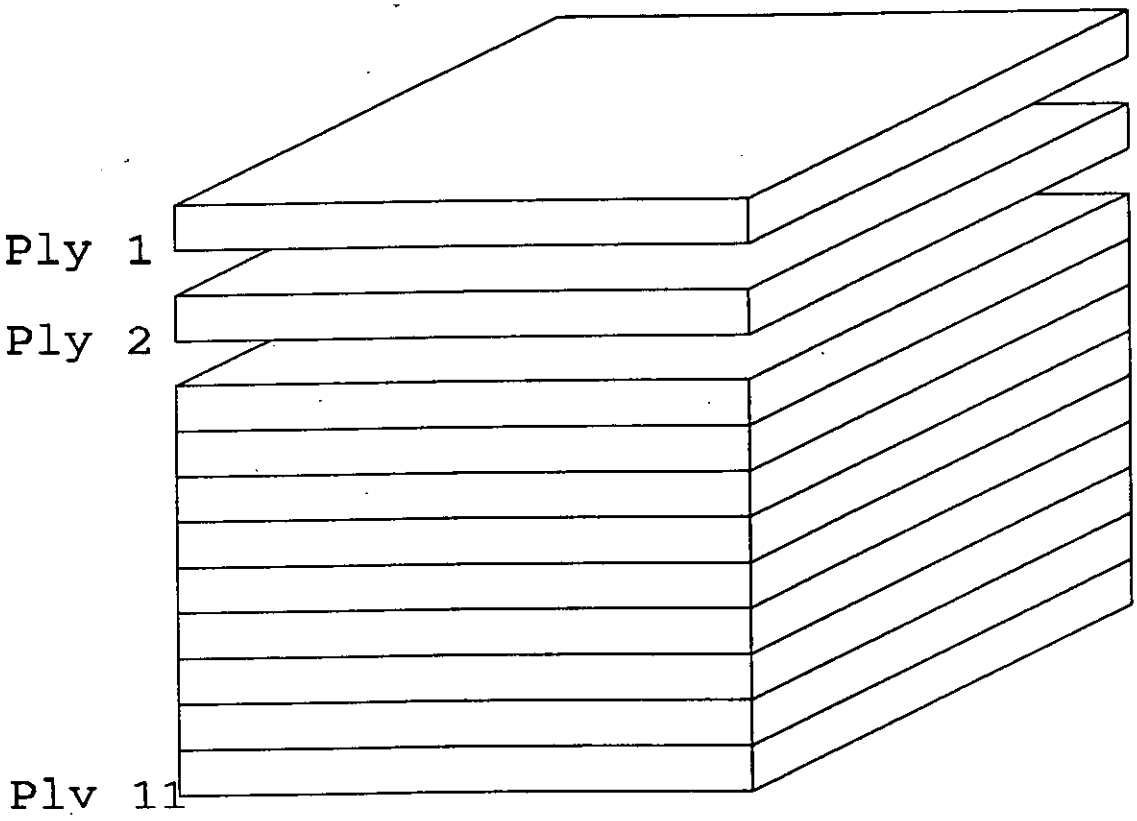

FIGURE 10a. The effect of location of the second delamination on the stiffness of a laminate which has the first delamination below ply 1.

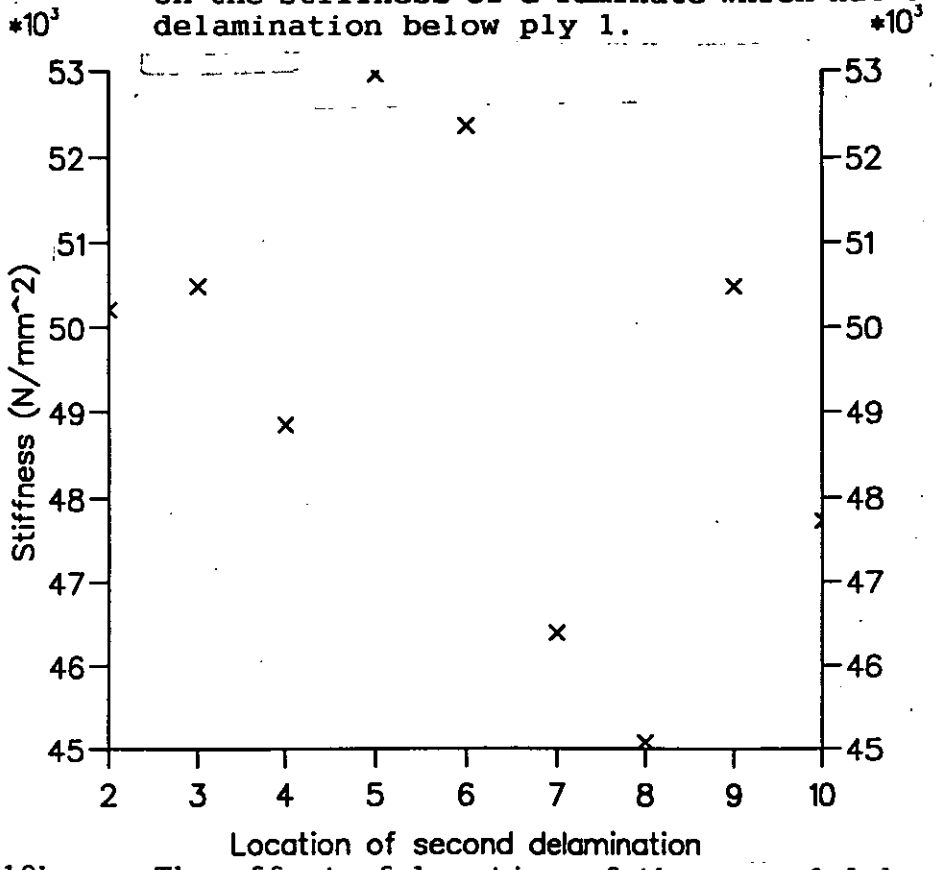

FIGURE 10b. The effect of location of the second delamination on the critical strain of a laminate which has the first delamination below ply 1.

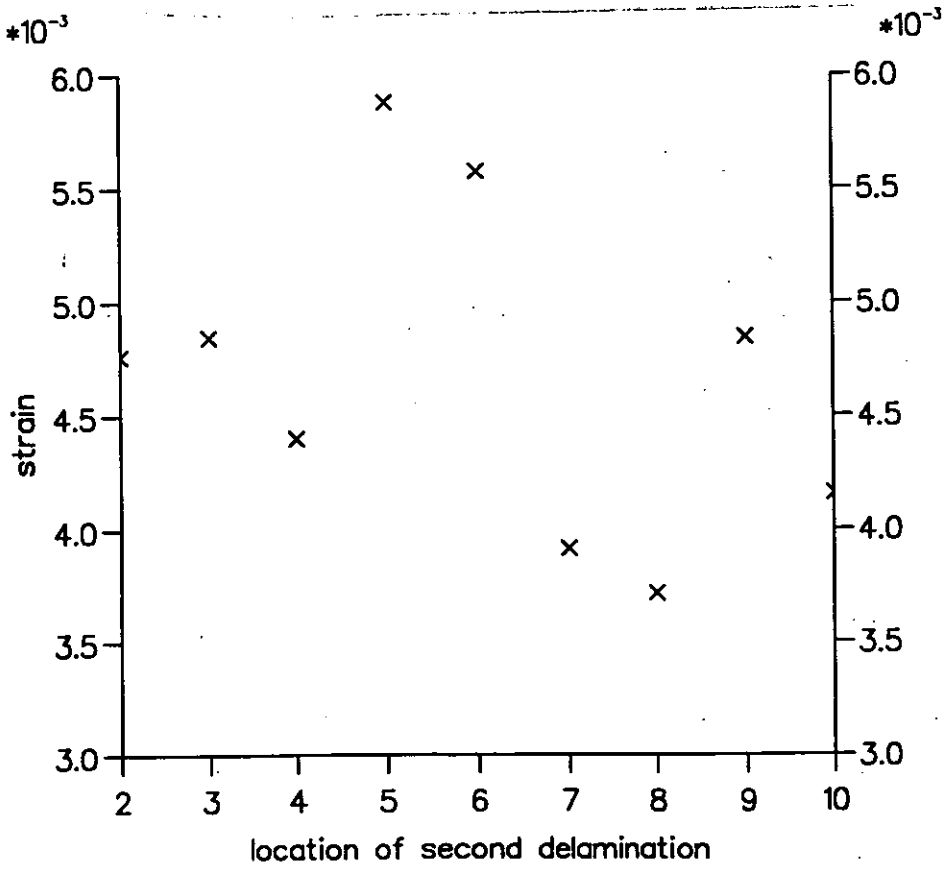

FIGURE 11a. The effect of location of the second delamination on the stiffness of a laminate which has the first delamination below ply 2.

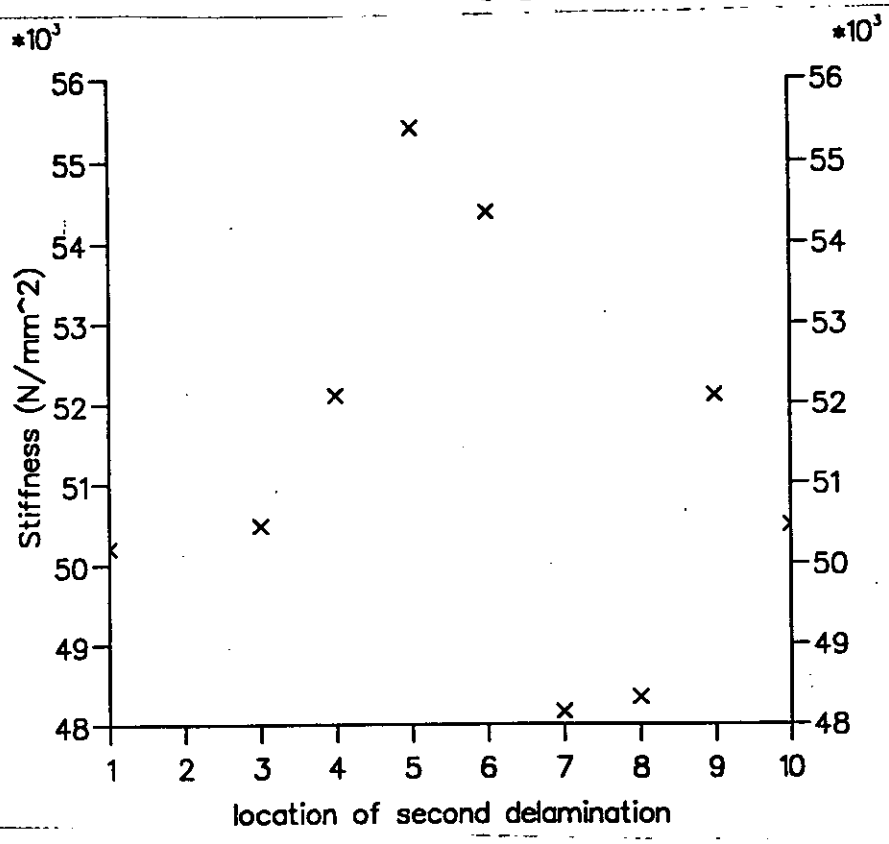

FIGURE 11b. The effect of location of the second delamination on the critical strain of a laminate which has the first delamination below ply 2.

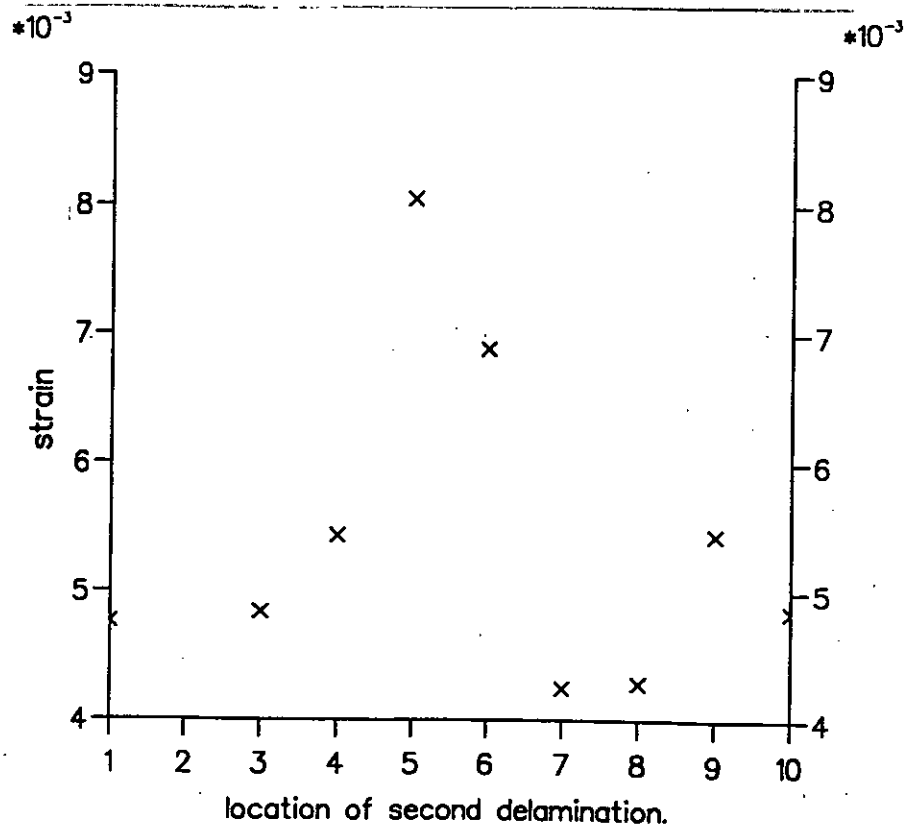

FIGURE 12a. The effect of location of the second delamination on the stiffness of a laminate which has the first delamination below ply 3.

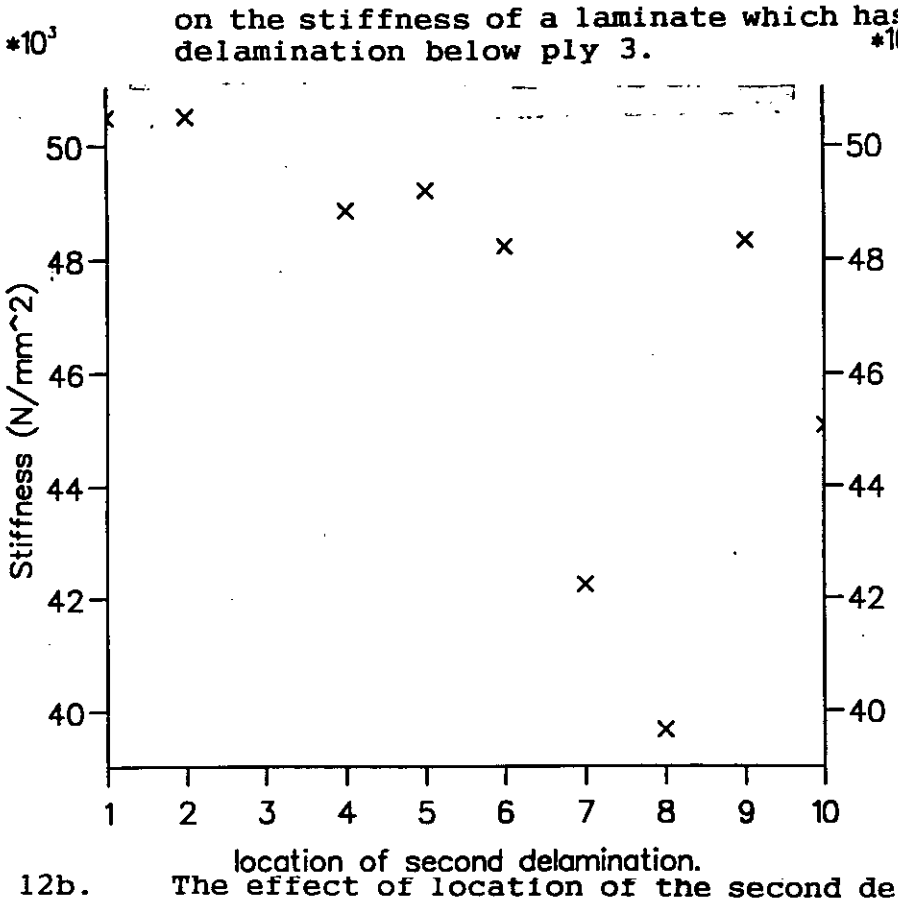

FIGURE 12b. The effect of location of the second delamination on the critical strain of a laminate which has the first delamination below ply 3.

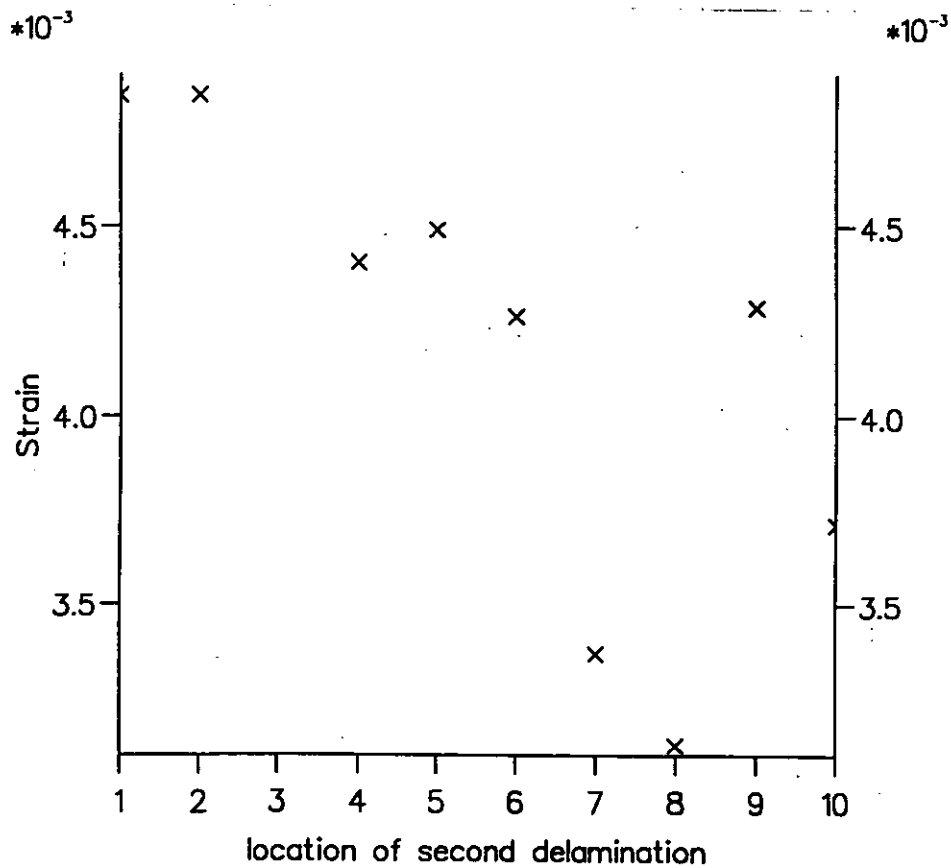

FIGURE 13a. The effect of location of the second delamination on the stiffness of a laminate which has the first delamination below ply 4.

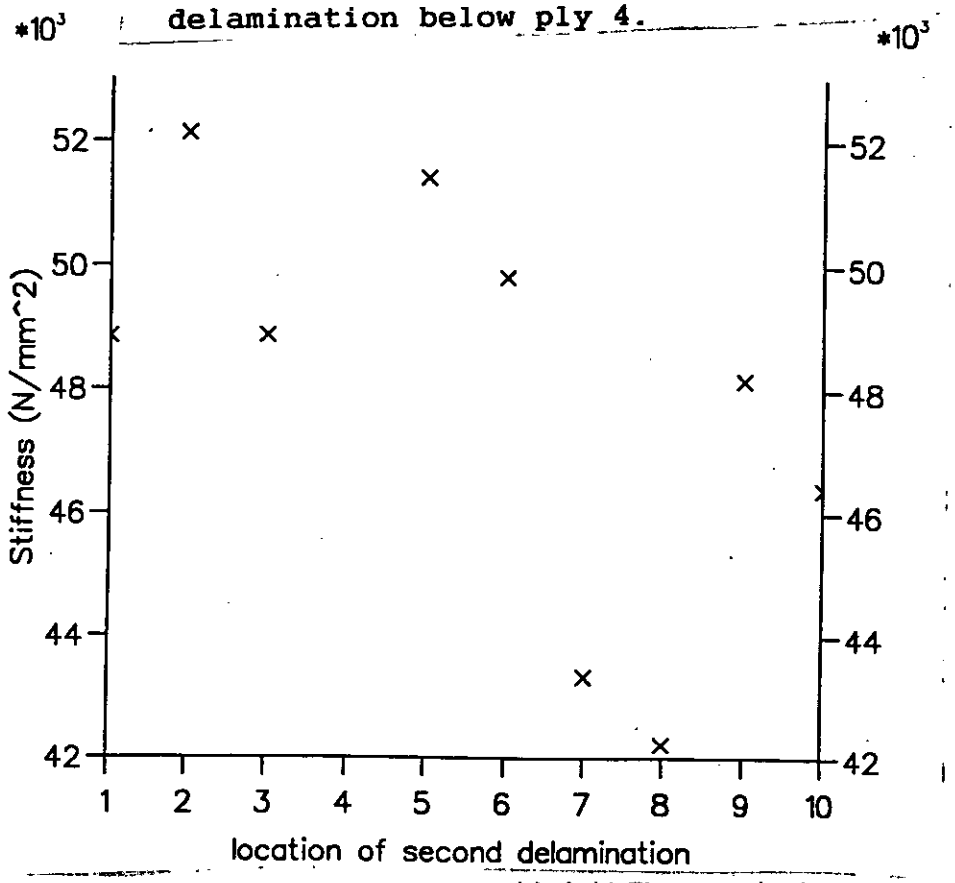

FIGURE 13b. The effect of location of the second delamination on the critical strain of a laminate which has the first delamination below ply 4.

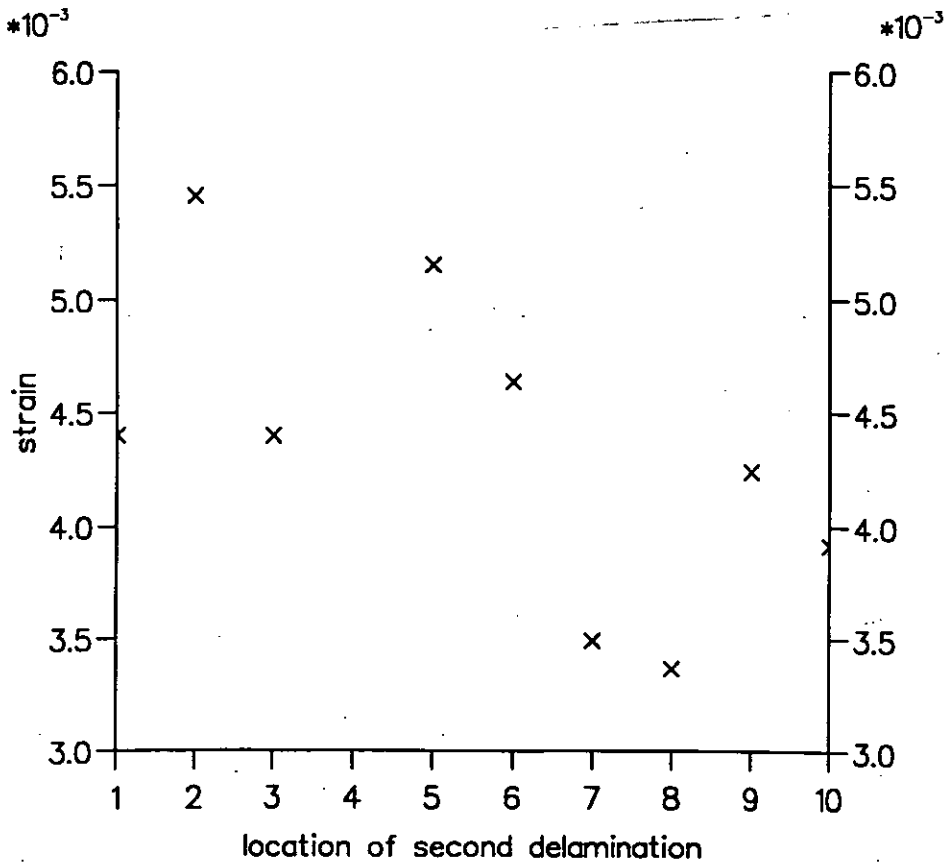

FIGURE 14a. The effect of location of the second delamination on the stiffness of a laminate which has the first delamination below ply 5.

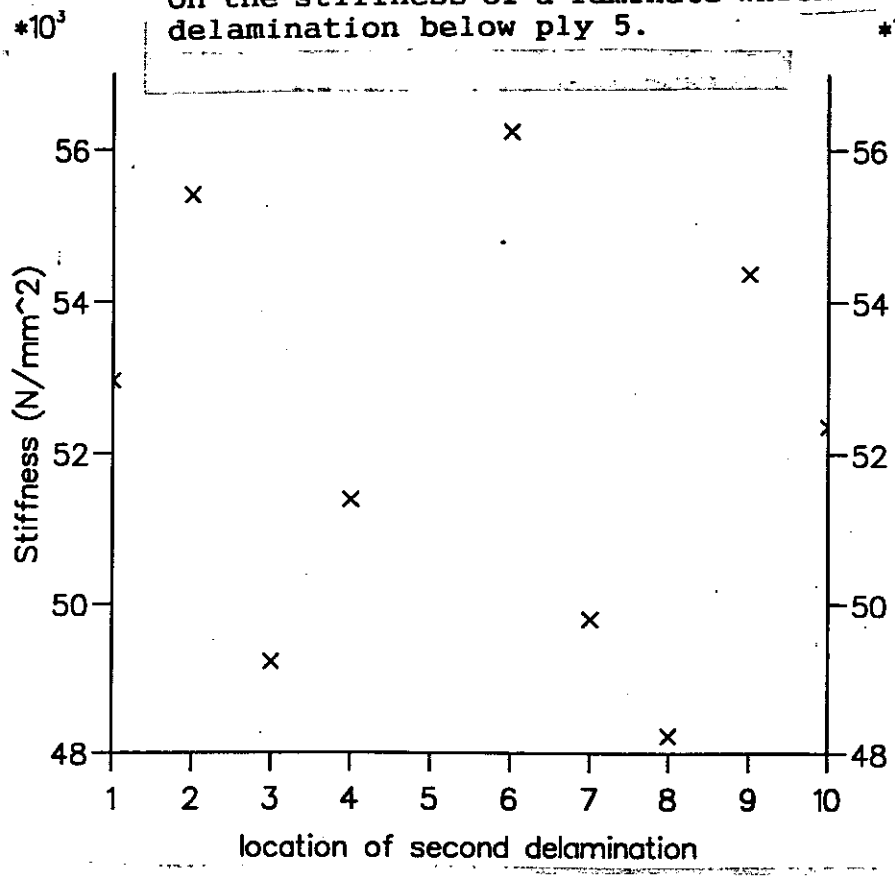

FIGURE 14b. The effect of location of the second delamination on the critical strain of a laminate which has the first delamination below ply 5.

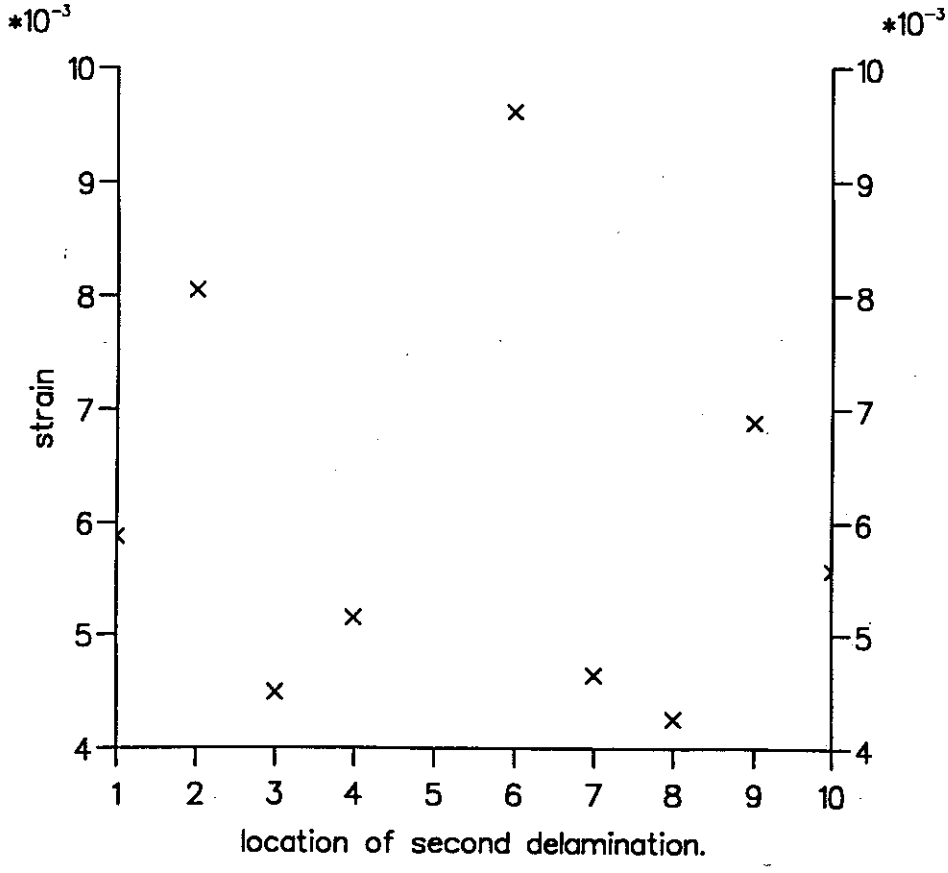

FIGURE 15. Plot of the function given in equation (8) for different values of λ.

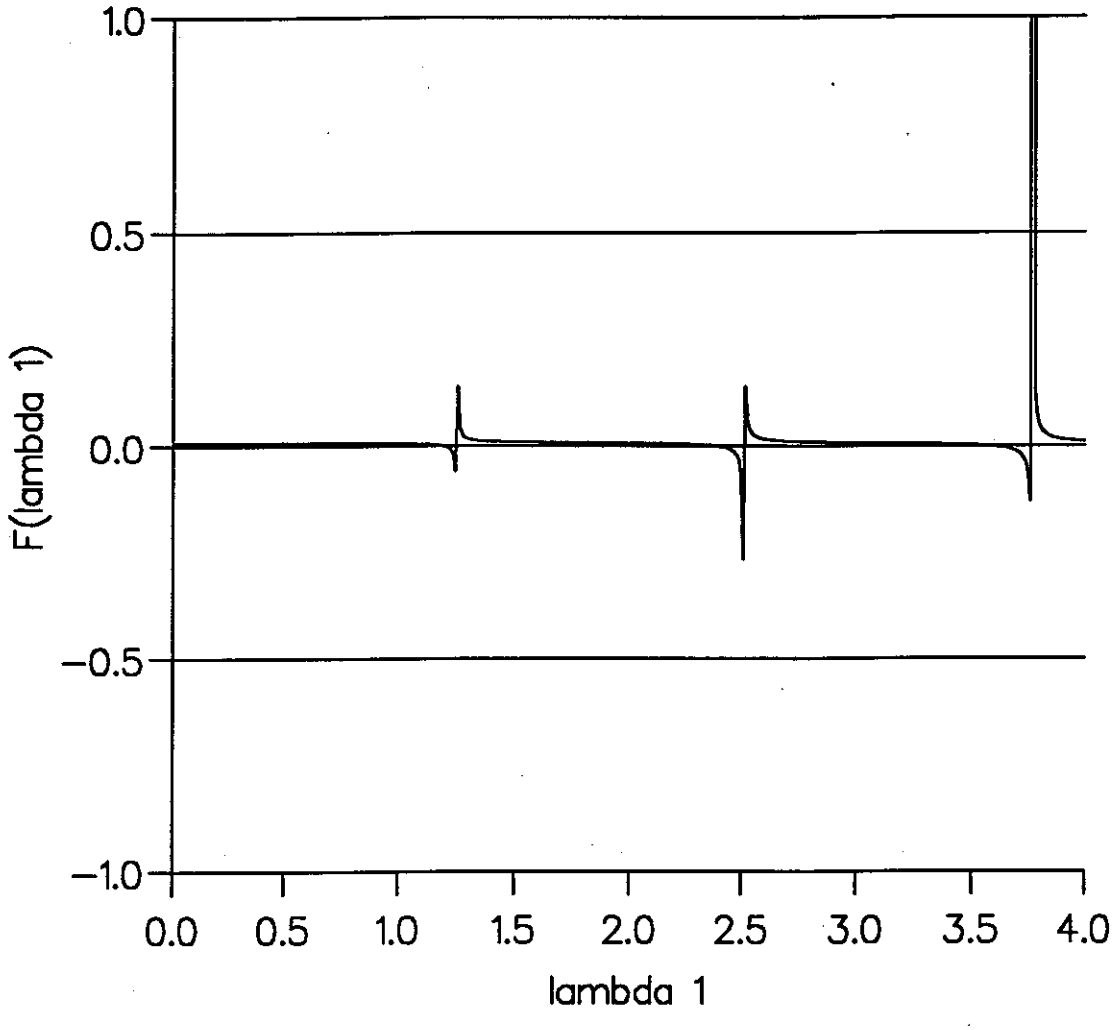

FIGURE 16. Critical buckling stress against delamination length.

T2/T3=1.0; L=3; T1=0.22

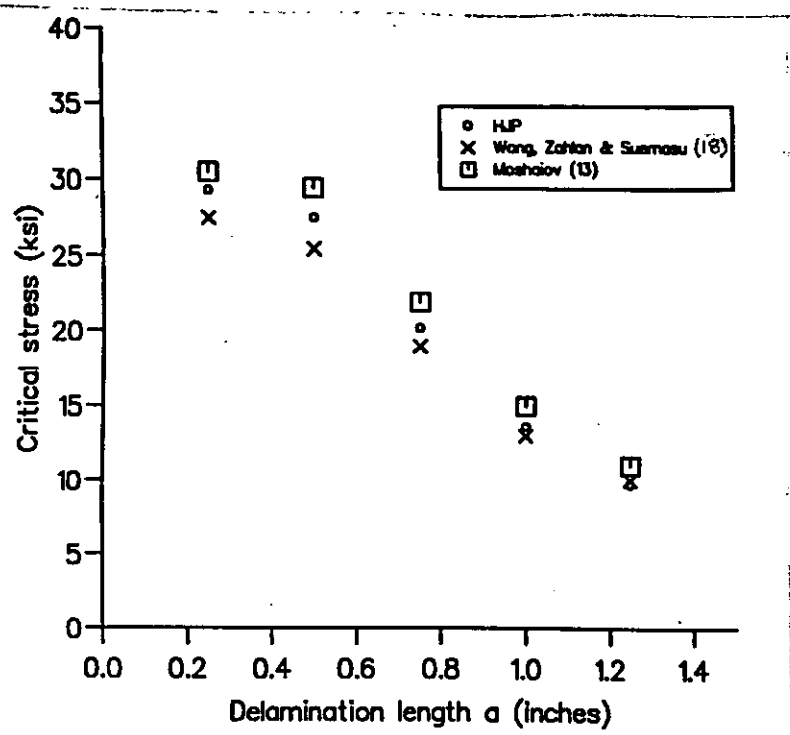

FIGURE 17. Critical buckling stress against delamination length for different values of E, the laminate stiffness.

T2/T3=1.0; L=3; T1=0.22

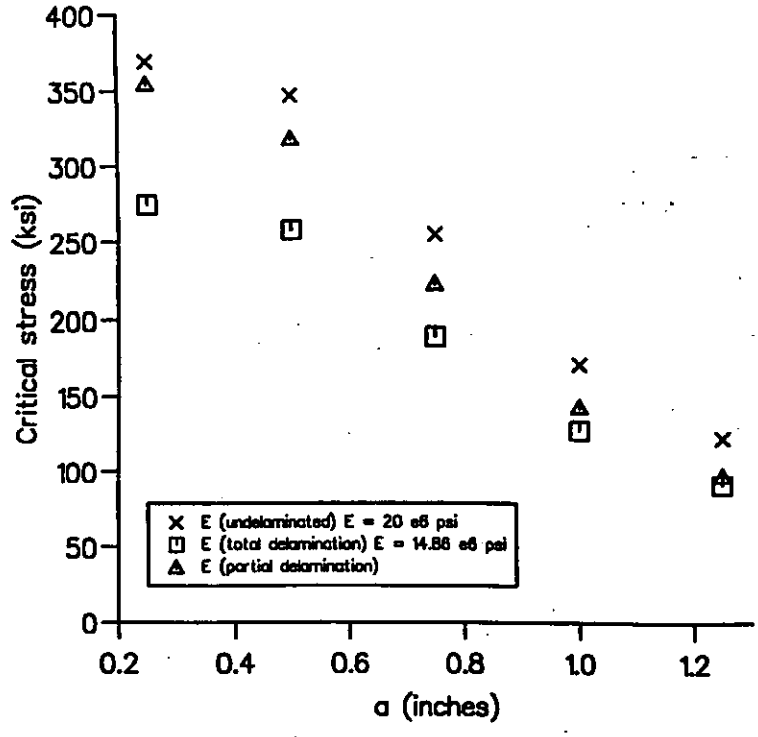

FIGURE 18. Critical buckling stress against delamination length for different through-thickness location of delamination.

T1=0.22"; L=3".

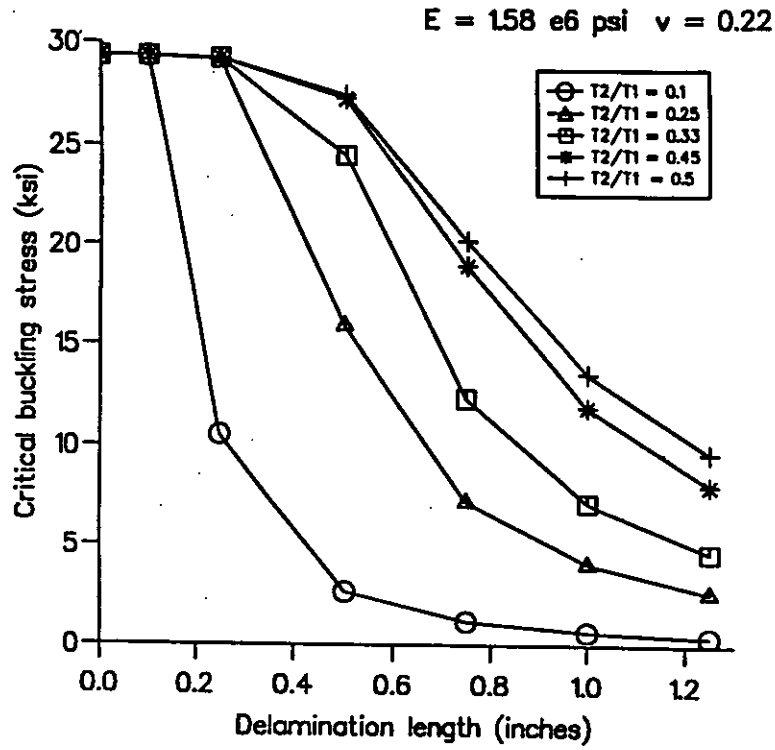

FIGURE 19. Critical buckling stress against delamination length for different laminate thicknesses. The delamination is assumed to be at mid-depth.

L=3".

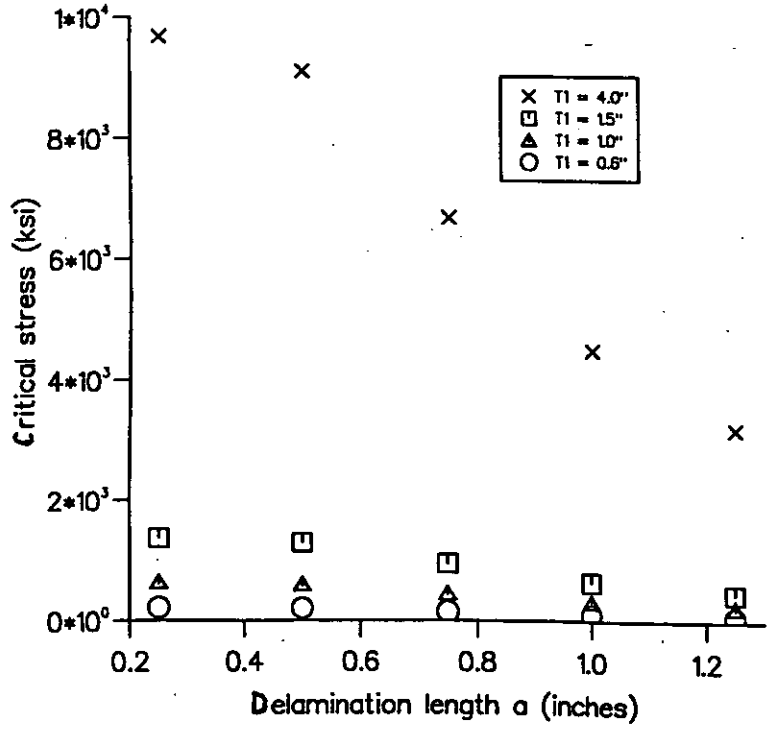

FIGURE 20. Critical buckling stress against plate thickness for different delamination lengths. The delamination is assumed to be at mid-depth.

L=3".

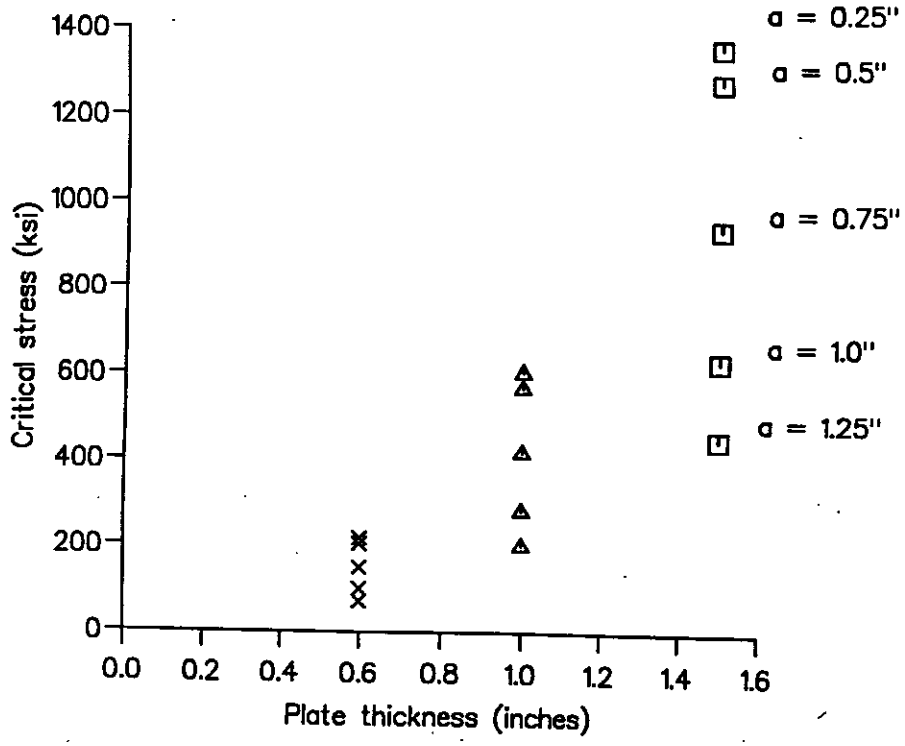

FIGURE 21a. Critical stress against defect length.
Hand lay-up specimens.
T_3=0.8 mm.

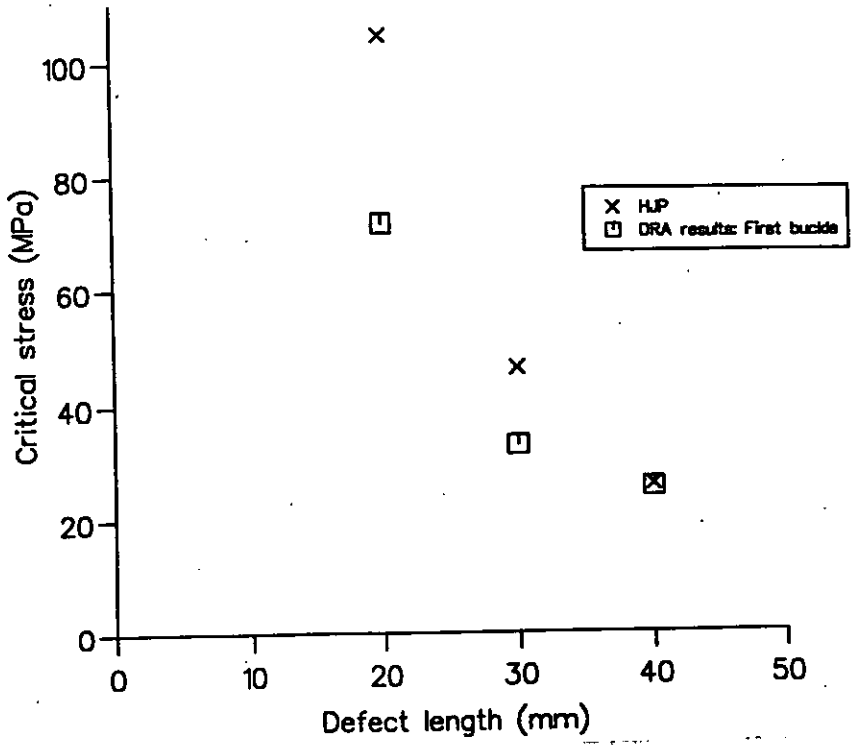

FIGURE 21b. Critical stress against defect length.
Hand lay-up specimens.
T_3=1.7 mm.

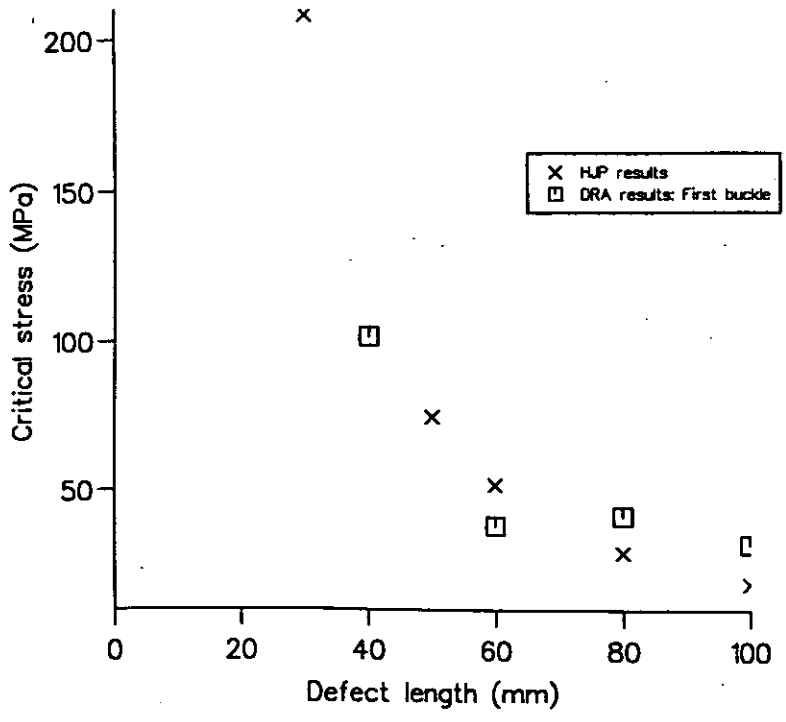

FIGURE 21c. Critical stress against defect length. Hand lay-up specimens. T_3=2.5 mm.

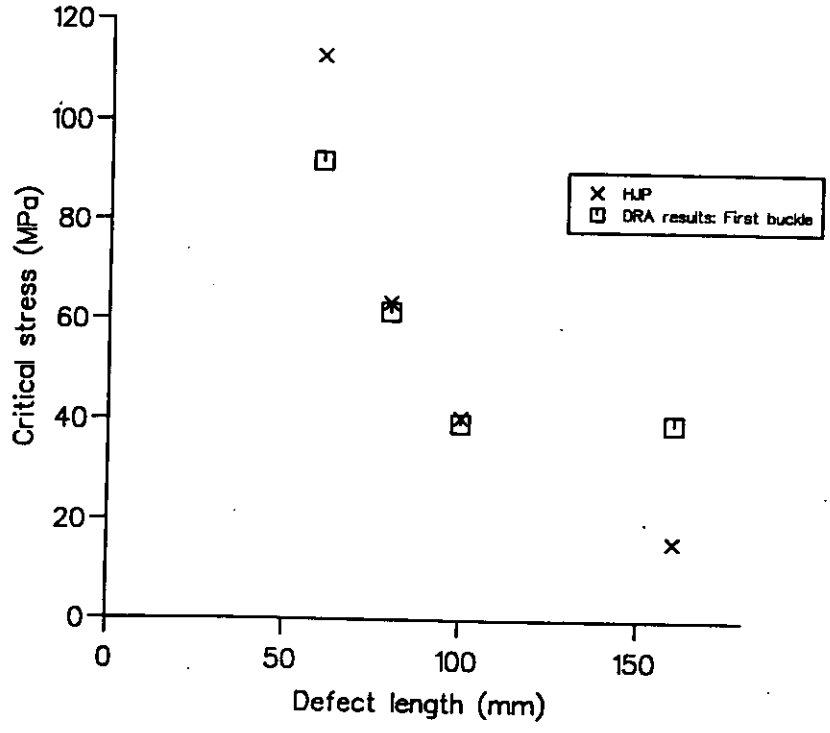

FIGURE 21d. Critical stress against defect length. Hand lay-up specimens. T_3=3.3 mm.

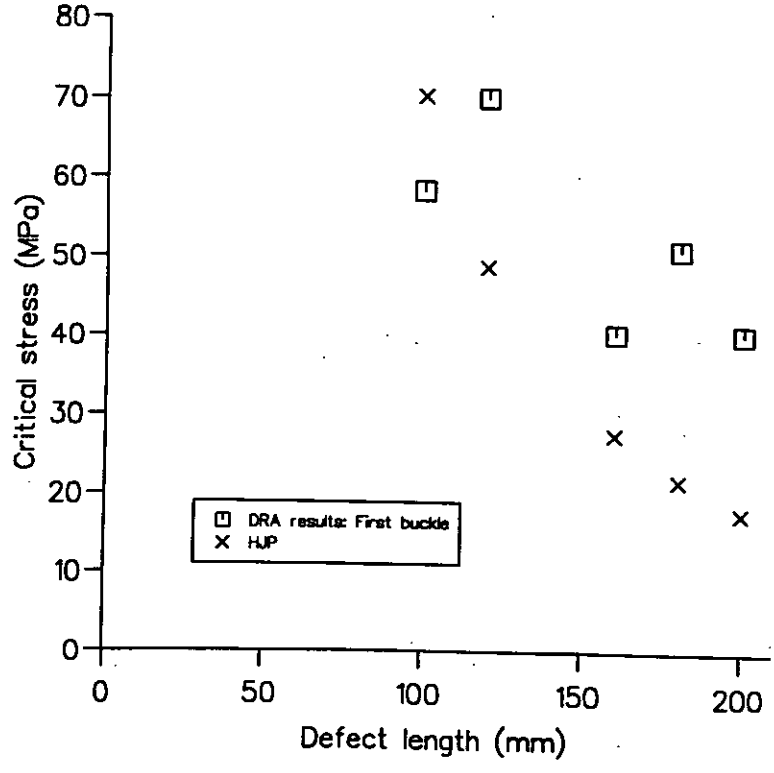

FIGURE 21e. Critical stress against defect length. Hand lay-up specimens. T_3=4.2 mm.

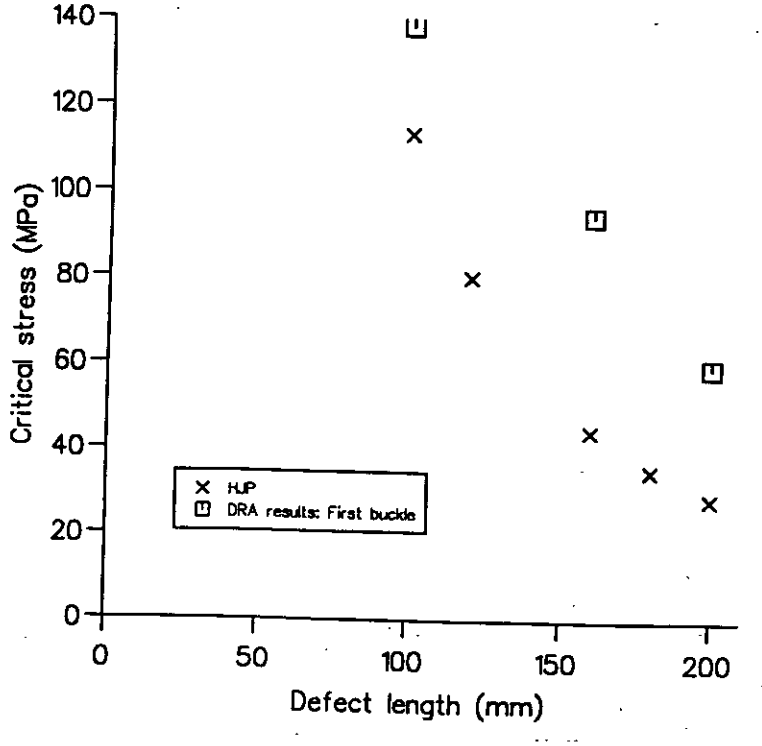

FIGURE 22a. Critical stress against defect length. V.R.T. specimens. T_3=0.53 mm.

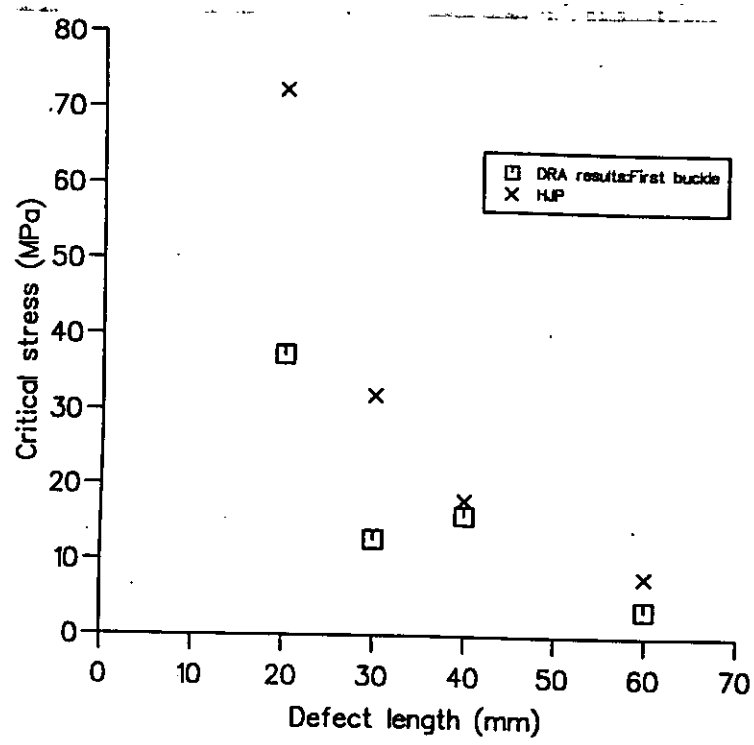

FIGURE 22b. Critical stress against defect length. V.R.T. specimens. T_3=1.06 mm.

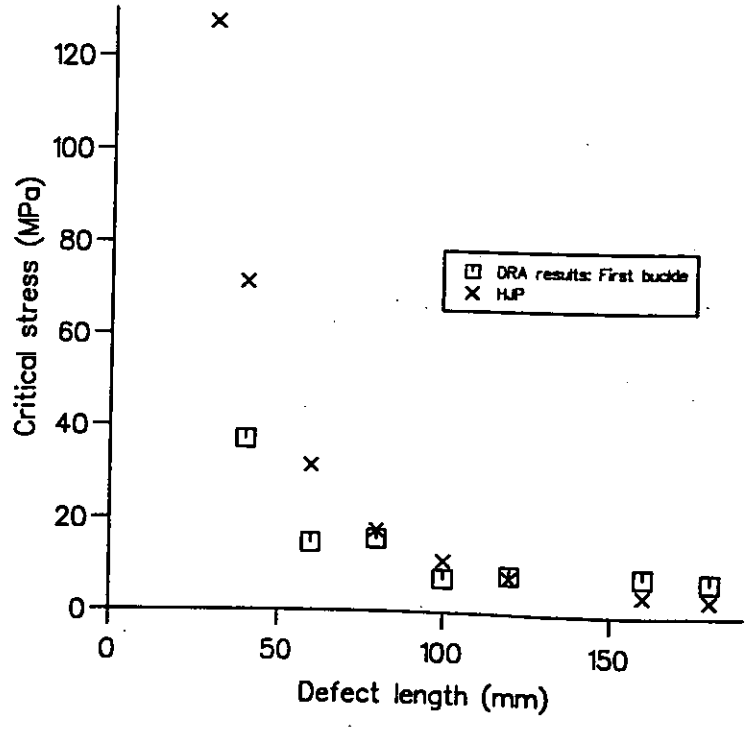

FIGURE 22c. Critical stress against defect length. V.R.T. specimens. T_3=1.59 mm.

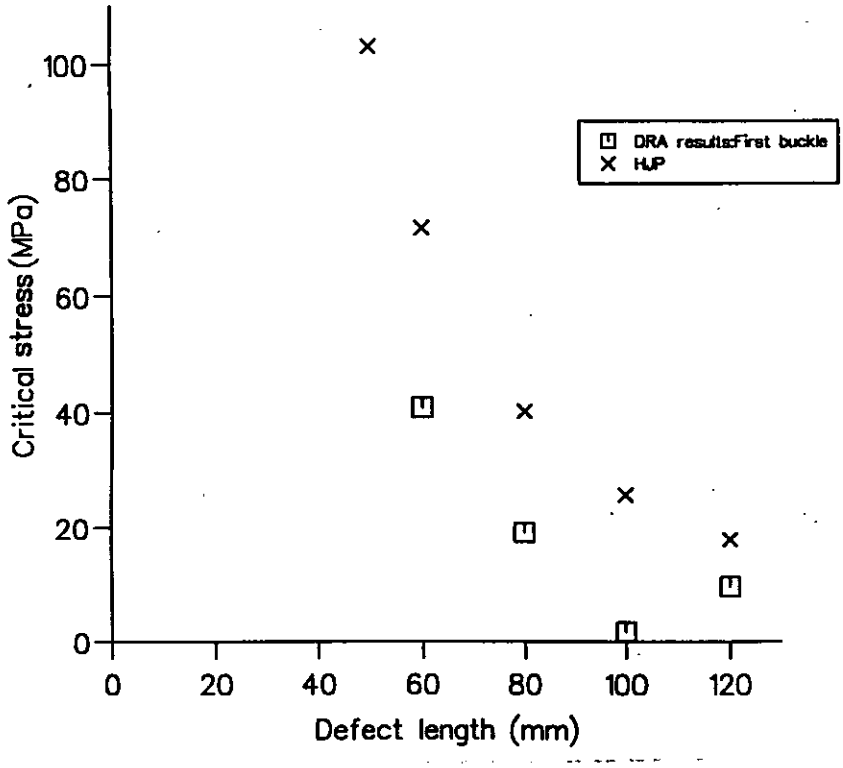

FIGURE 22d. Critical stress against defect length. V.R.T. specimens. T_3=2.12 mm.

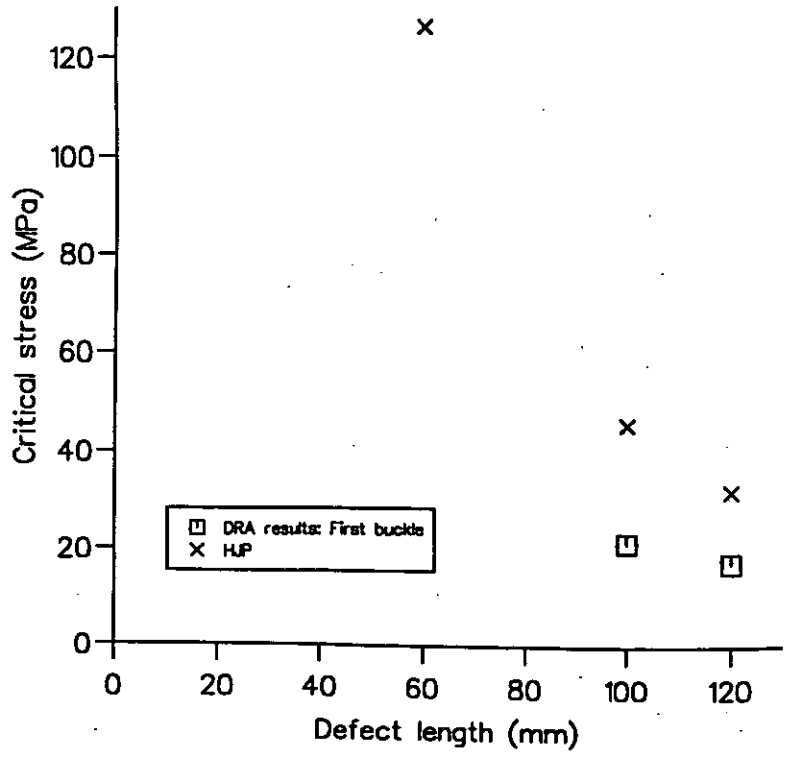

FIGURE A1. Laminate containing complete delaminations.

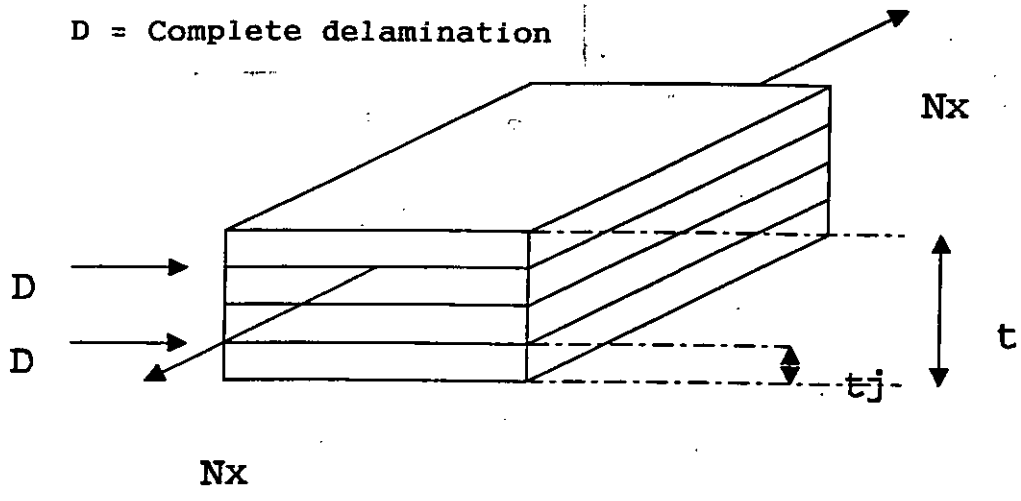

FIGURE A2. Laminate containing partial (edge) delaminations.

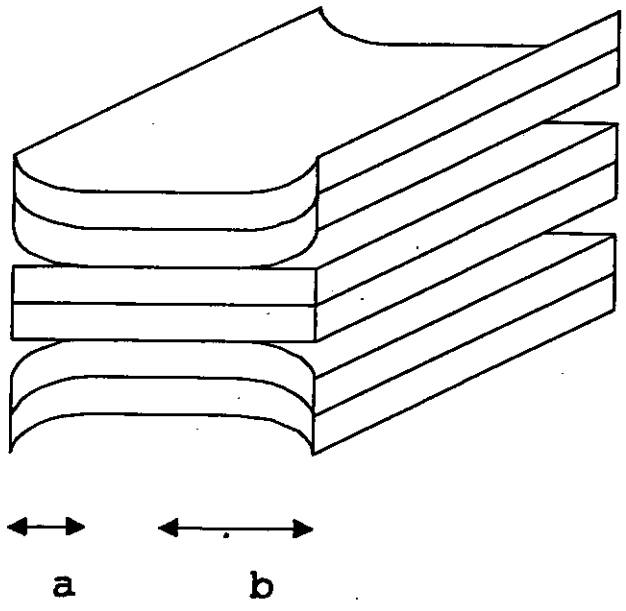

FIGURE B1. Sign conventions for positive moments and forces.

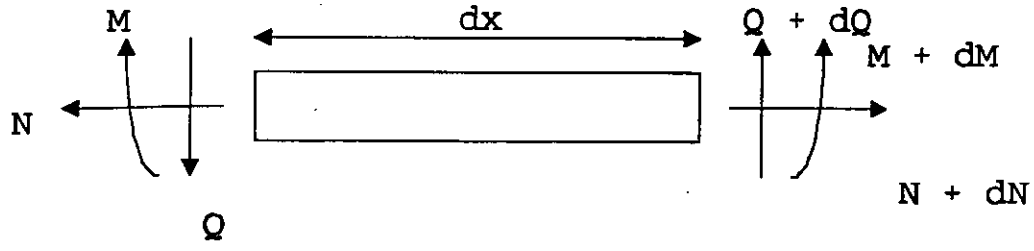

FIGURE B2. Forces and moments acting on a column element in a deformed configuration.

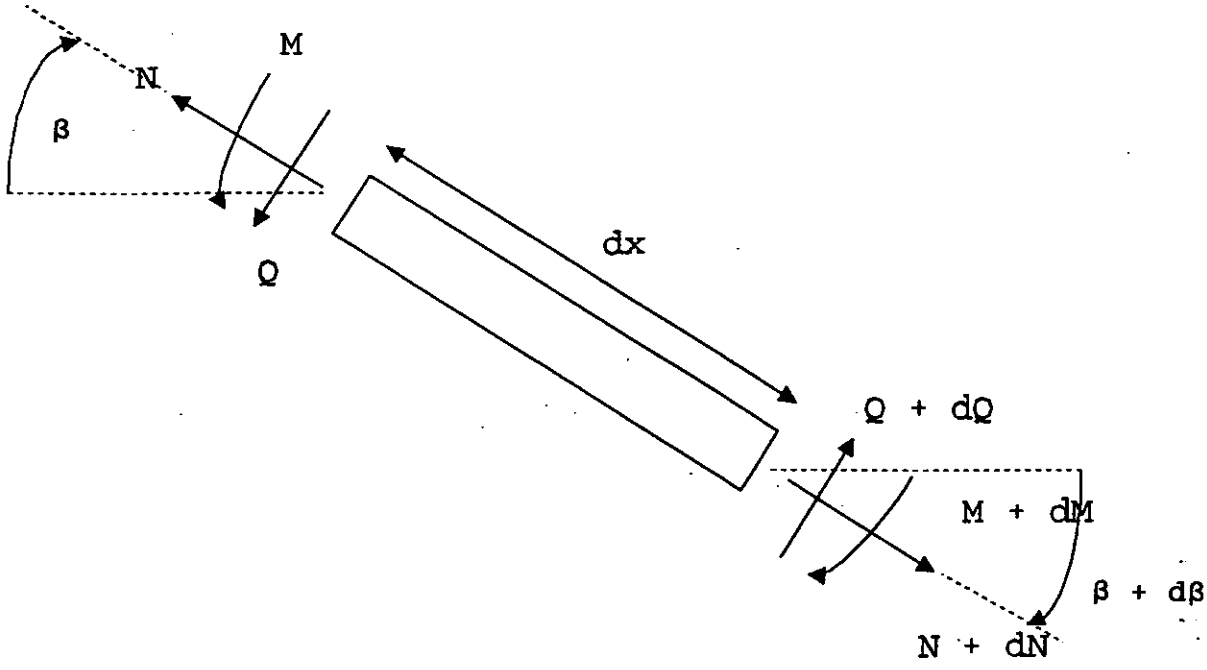

FIGURE B3. Forces acting on parts 2 and 3 of a delaminated beam.